INTERPLANETARY SHOCK WAVES AND THE STRUCTURE OF SOLAR WIND DISTURBANCES

A. J. Hundhausen

An invited review

ABSTRACT

Observations and theoretical models of interplanetary shock waves are reviewed with emphasis on the large-scale characteristics of the associated solar wind disturbances and on the relationship of these disturbances to solar activity. The sum of present day observational knowledge indicates that shock waves propagate through the solar wind along a broad, roughly spherical front, ahead of plasma and magnetic field ejected from solar flares. Typically, the shock front reaches 1 AU about two days after its flare origin, and is of intermediate strength (Mach number of ~2). Not all large flares produce observable interplanetary shock waves; the best indicator of shock production appears to be the generation of *both* type II and type IV radio bursts by a flare. Theoretical models of shock propagation in the solar wind can account for the typically observed shock strength, transit time, and shape. Both observations and theory imply that the flare releases a mass of $\sim 5 \times 10^{16}$ gm and an energy of $\sim 1.6 \times 10^{32}$ ergs into the shock wave on a time scale of hours. This energy release estimate indicates that the shock wave is a major energy loss mechanism for some solar flares.

INTRODUCTION

The existence of interplanetary shock waves was inferred from the short rise times of geomagnetic sudden impulses [*Gold*, 1955] before the era of direct interplanetary observations. Quantitative theoretical models of shock propagation through an ambient interplanetary medium were shortly thereafter developed by *Parker* [1961]. Since the first direct observation of such a shock by the Mariner 2 spacecraft in 1962 [*Sonett et al.*, 1964], considerable effort, both theoretical and observational, has been directed to the study of interplanetary shock waves. Most of this effort has concentrated on the detailed, local characteristics of the shock front. In contrast, here we emphasize the relationship of interplanetary shocks to the large-scale solar wind disturbances of which they are part and to the solar activity thought to produce the entire phenomenon. For purposes of this discussion the following terminology is used: *shock* is the surface discontinuity at which plasma properties change abruptly; a *solar wind disturbance* is any large-scale perturbation of ambient or quiet solar wind conditions; a *shock wave* is a solar wind disturbance with a shock at its leading edge. These phenomena are discussed in reviews by *Wilcox* [1969] and *Hundhausen* [1970*a*, *b*].

A QUALITATIVE DESCRIPTION OF SOLAR WIND DISTURBANCES

Classical studies of solar-terrestrial relationships have pointed to the existence of two classes of interplanetary disturbances: transient disturbances following some solar flares, and recurrent (at 1 AU) disturbances thought to be produced by long-lived active regions (the so-called "M regions"). We present here qualitative descriptions of the interactions (leading to the formation of shocks) of these two types of disturbances with a steady, spherically symmetric, ambient solar wind. These descriptions will prove useful in organizing later discussions of quantitative theoretical models and of shock observations.

This paper was prepared while the author was at the University of California Los Alamos Scientific Laboratory, Los Alamos, New Mexico. Present Address is High Altitude Observatory, National Center for Atmospheric Research, Boulder, Colorado.

Figure 1 illustrates the plasma and magnetic field characteristics expected in a steady, structureless solar wind near the solar equatorial plane. At heliocentric distances greater than 10 to $20R_{\odot}$, solar wind models predict an almost radial plasma flow at nearly constant speed [*Parker,* 1963, 1969]. The expansion of the highly conductive plasma and the rotation of the sun combine to produce the familiar spiral pattern of the interplanetary magnetic field lines [*Parker,* 1963, pp. 137–138]. Figure 1(*a*) shows the plasma and field configuration in a frame of reference stationary with respect to the solar system. Figure 1(*b*) shows the same configuration in a frame of reference rotating with the sun; in this latter frame both the field lines and flow streamlines are Archimedes spirals for a constant expansion speed.

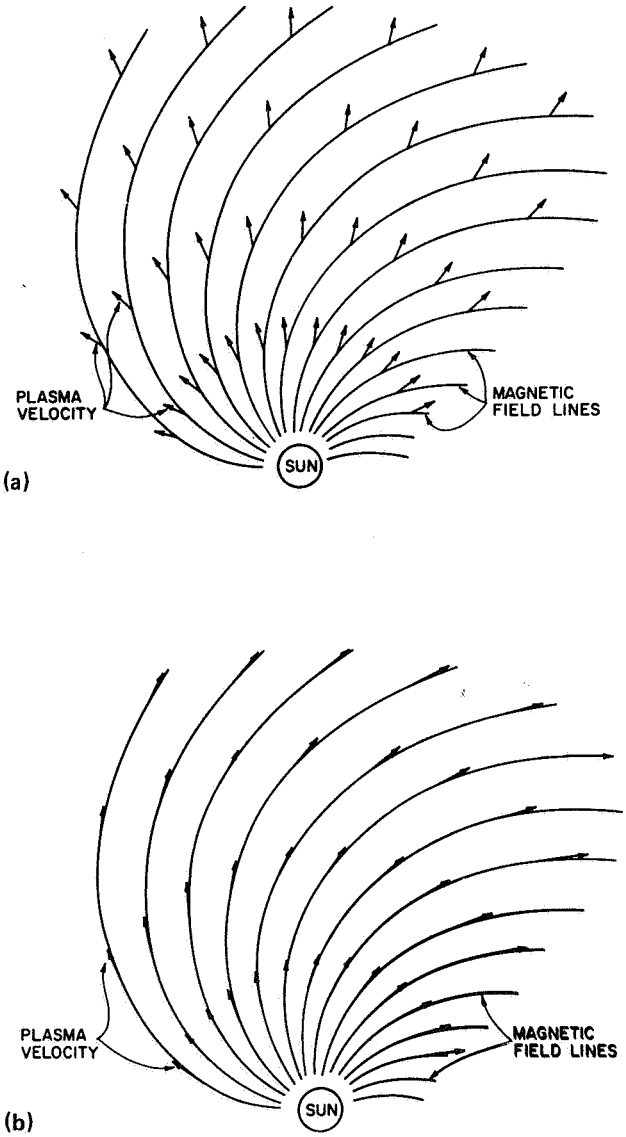

Figure 1. *The plasma flow and magnetic field line configurations near the solar equatorial plane for a spherically symmetric, steady solar wind. Part (a) shows the flow pattern in a stationary frame of reference, while part (b) shows the same pattern in a frame of reference rotating with the sun.*

Flare-Associated Solar Wind Disturbances

Optical, radio, particle observations all indicate that material is explosively ejected by large solar flares. Consider a volume of this material, presumably plasma from the chromosphere or low corona, moving rapidly outward into a slower ambient solar wind. Figure 2 shows a hypothetical cross section (in the solar equatorial plane) of the resulting solar wind disturbance at a time when it has traveled well out into interplanetary space. The shape given the disturbance in the drawing assumes some lateral expansion; theoretical and observational arguments for this effect are given in later sections. The ambient solar wind plasma and magnetic field lines must be compressed and pushed aside by expanding flare ejecta (the high electrical conductivity of the plasma prevents rapid interpenetration of the plasmas). If the speed of the ejected material exceeds the ambient solar wind speed by more than the local sound (or Alfvén) speed, a shock front will form at the leading edge of the compressed ambient plasma shell.

The nature of the boundary between the compressed ambient solar wind and the flare ejecta depends somewhat on details of the flare process. If the flare region was also a source of the ambient solar wind, the magnetic field lines in the flare plasma must connect to the ambient field. However, for the configuration shown in figure 2, this connection would take place only on a small part of the boundary, as shown just above and to the right of the flare site. Most of the boundary surface separates plasmas from different solar source regions, as well as with different time histories. Thus, the material on the two sides of the boundary might be expected to have different thermodynamic and chemical properties. Further, magnetic field lines would not cross such a region of the boundary, which must then form a tangential discontinuity within the interplanetary plasma and magnetic field [*Colburn and Sonett,* 1966]. If the flare region was not a source of the ambient solar wind, the *entire* boundary surface would separate plasma from different source regions and would be expected to be a tangential discontinuity; this situation is entirely different from that illustrated by *Parker* [1963] for a

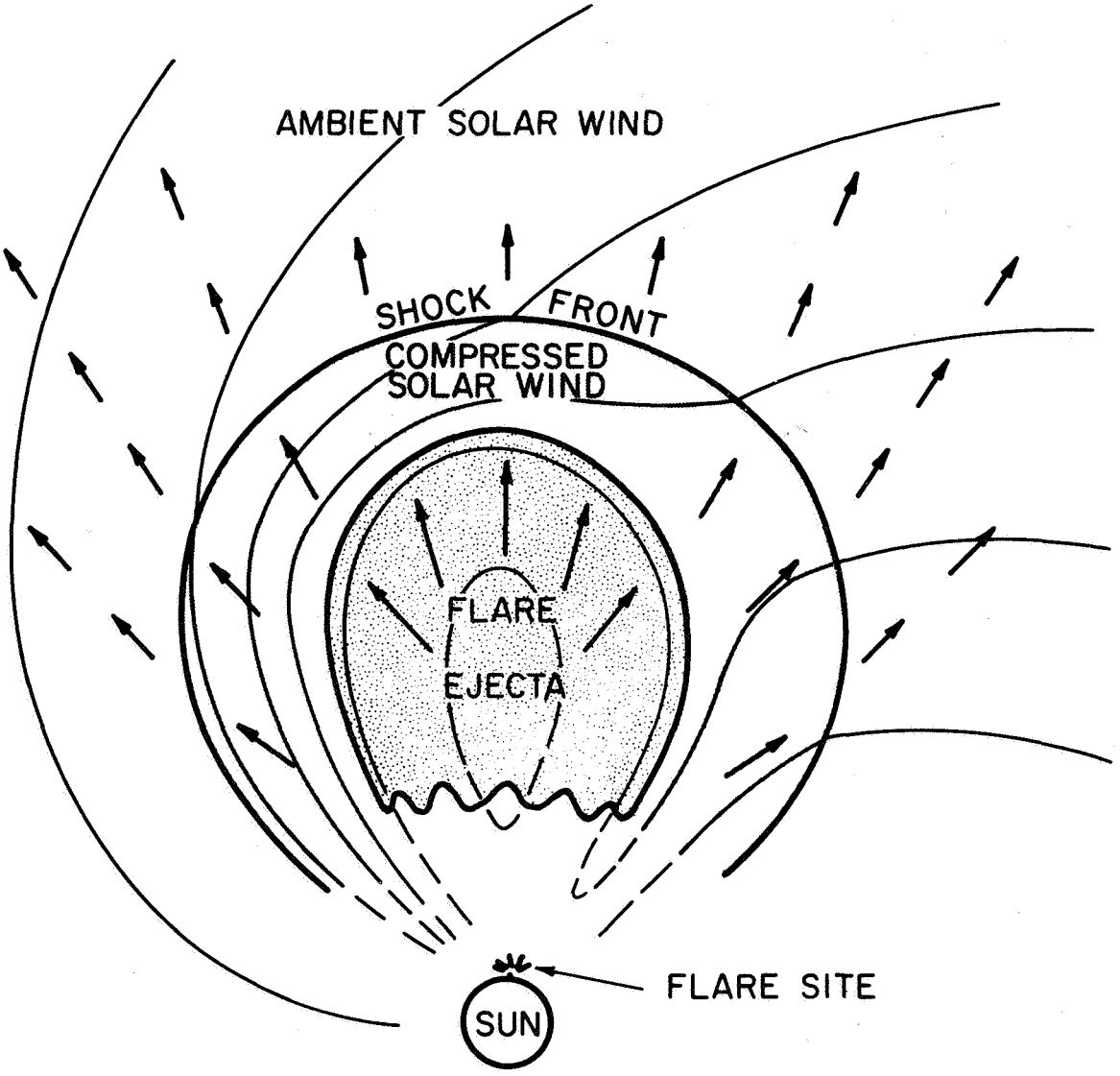

Figure 2. *A qualitative sketch, in equatorial cross section, of a flare-produced solar wind disturbance, propagating into an ambient solar wind similar to that shown in figure 1. The arrows again indicate the plasma flow velocity and the light lines indicate the magnetic field. The rotation of the sun has been neglected in drawing a configuration symmetric about the flare site.*

spherically symmetric wave, where the entire boundary is crossed by the field lines [*Colburn and Sonett*, 1966]. The rarity of collisions in the tenuous interplanetary plasma leads to extremely slow diffusion normal to magnetic field lines. The expected tangential nature of the boundary discontinuity would then help to preserve any thermodynamic or chemical differences between the ambient and flare plasmas.

The magnetic field and plasma structure within the flare ejecta depends strongly on the details of the flare process. The magnetic field lines must connect back to the flare site (with a current sheet extending through the body of the ejecta as well as along its boundary) unless some diffusion of the plasma relative to the field lines, or "reconnection" of the field lines [*Petschek*, 1966] were to occur. Reconnection is a distinct possibility, as some theories of solar flares employ this process as the basic flare mechanism; for example, figure 3 shows the magnetic field configurations assumed and produced in the flare model of *Sturrock* [1967]. Such reconnection would produce closed magnetic loops within the flare plasma, as shown by the dashed field line of figure 2.

This configuration has been advocated by Gold [see the numerous discussions following relevant papers in *Mackin and Neugebauer,* 1966]. If some of the ejected material moves outward more rapidly than that near the tangential discontinuity (due either to acceleration of the former or deceleration of the latter) a second shock might form within the flare ejecta. This would be a "reverse" shock, moving toward the sun relative to the plasma but convected outward by the rapid plasma motion [*Sonett and Colburn,* 1965].

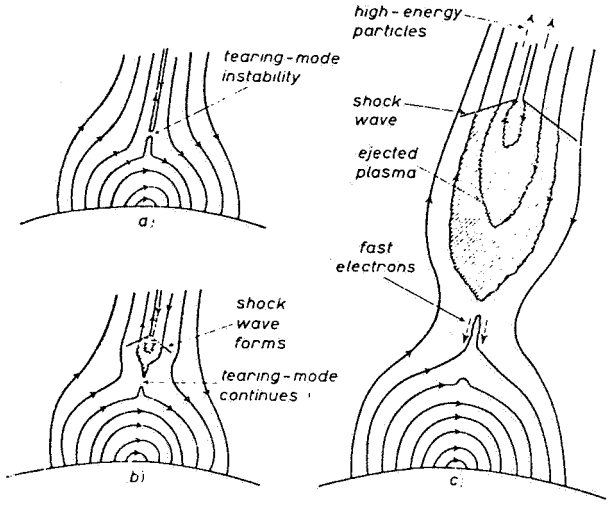

Figure 3. *Coronal magnetic field configurations in the solar flare model of Sturrock [1967]. Closed magnetic field loops are formed within the flare ejecta (c) by the field line reconnection process taken to be the basic energy mechanism in the model.*

Steady, High-Speed Solar Wind Streams

Solar wind observations such as those by *Neugebauer and Snyder* [1966] indicate that some streams of high speed solar wind, presumably emanating from specific centers of solar activity, persist long enough to be present on several successive solar rotations. Consider such a steady stream of solar wind flowing radially outward, with high, constant speed, from a source rotating with the sun. Figure 4 shows a hypothetical cross section of this stream (in the solar equatorial plane) viewed in the frame of reference rotating with the sun. In this frame, as in figure 1(*b*), the flow is along Archimedes spirals, with the magnetic field lines along the flow streamlines. The flow of a slow ambient wind, assumed to exist ahead of the fast stream, is along more tightly wound spirals that must eventually intersect the high speed stream. The high electrical conductivity of the plasma again prevents interpenetration, and the ambient plasma must be compressed and deflected to ultimately flow parallel to the interface with the fast stream. If the inflow of the ambient plasma relative to this interface exceeds the local sound speed, a shock wave should form at the leading edge of the compressed ambient plasma region. The resulting flow pattern is steady in the frame of reference rotating with the sun. Figure 5 shows this pattern transformed into a stationary frame of reference, wherein the entire shock wave would appear to rotate counterclockwise about the sun.

The structure of the magnetic field and plasma in this shock wave is, in many ways, similar to that already described for flare-associated disturbances. The boundary between the compressed ambient solar wind and the high speed stream should again be a tangential discontinuity separating plasma and magnetic fields from two different solar source regions. The material on the two sides of the boundary might again be expected to have different thermodynamic and chemical properties, preserved because of the slow rates of diffusion across the field lines. A second or reverse shock could again form within the high speed stream if material is flowing toward the tangential discontinuity [*Colburn and Sonett,* 1966].

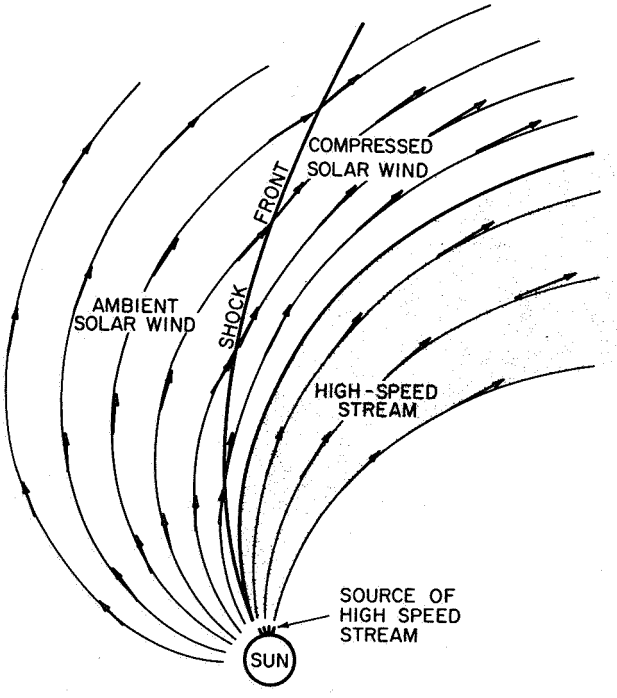

Figure 4. *A qualitative sketch, in equatorial cross section, of a steady, localized stream of high speed solar wind interacting with a slow, ambient solar wind similar to that shown in figure 1. The interaction is shown in a frame of reference rotating with the sun. The arrows again indicate the plasma flow velocity and the light lines indicate the magnetic field.*

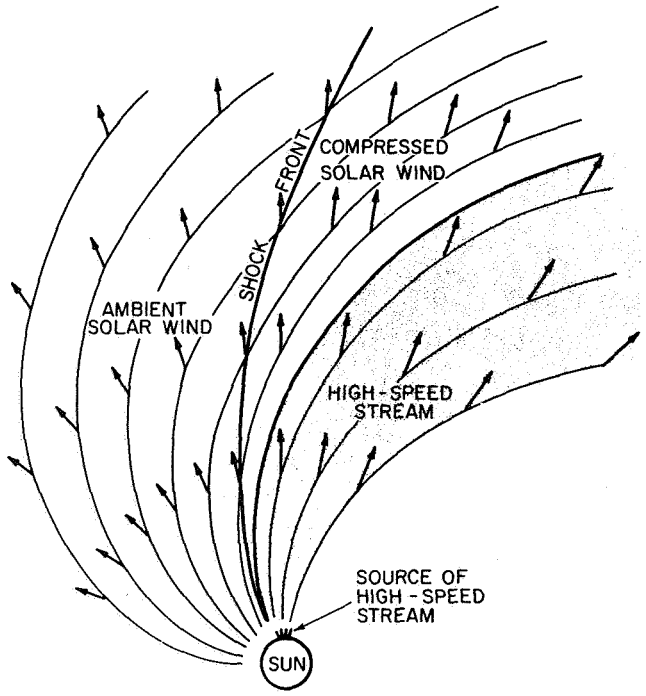

Figure 5. *The interaction of figure 4, shown here in a stationary frame of reference.*

Distinctions Between Flare-Associated and Steady-Stream Solar Wind Disturbances

Despite the many similarities between the flare-associated solar wind disturbance of figure 2 and the steady-stream disturbance of figure 5, several differences exist that might permit an observational distinction between the two classes. The most obvious of these is the shape of the shock front. For flare-associated disturbances the shock front is expected to be roughly symmetric about the radial direction from the flare site, while for steady-stream disturbances the shock front is more nearly alined with the spiral interplanetary field lines. Observations of a single disturbance by several widely separated spacecraft, or the observation and statistical analysis of many shock orientations by a single spacecraft [*Hirshberg,* 1968] might be used to distinguish these two geometries. A still more fundamental difference exists in the basic topology of the field lines intersecting the shock front. For flare-associated disturbances the field lines in the preshock, ambient plasma all lead outward toward interstellar space, while for the steady-stream disturbance the field lines in the preshock, ambient plasma connect back to the sun. Observations of galactic cosmic rays, whose high energies make them tracers of large-scale magnetic field geometry, might be capable of distinguishing the two topologies.

In pursuing either of these suggested tests, as is done in a later section, one should always bear in mind that these two classes of disturbances are idealized extremes. Intermediate classes, in which plasma is emitted from a solar source for about the same time required for its transit to an observer, could well occur and would be expected to display configurations between these two extremes. Further, solar flares occur in active regions, and thus might occur preferentially near the sources of high-speed streams; a correlation of this basic nature has been reported by *Bumba and Obridko* [1969]. The transient disturbances produced by such flares would be distorted by the lack of symmetry in the ambient medium into a configuration quite different from that shown in figure 2. We present some evidence later that solar wind disturbances appearing to be flare associated also show some characteristics of steady-stream emission.

THEORETICAL MODELS OF SOLAR WIND DISTURBANCES

Quantitative theoretical models have been developed for some aspects of the solar wind disturbances qualitatively described in the preceding section. Most attention has concentrated on the propagation of flare-associated shock waves under the assumption of spherical symmetry; as such models have recently been reviewed in some detail [*Hundhausen,* 1970*b; Hundhausen and Montgomery,* 1971], only a brief summary of some useful results is given here. The present discussion will then focus on the propagation of nonspherical, flare-associated shock waves, on the formation of shock waves in steady-stream disturbances, and on the effect of the high thermal conductivity of interplanetary electrons on both classes of solar wind disturbances.

Flare-Associated Shock Waves

Theoretical models of transient disturbances propagating through an ambient solar wind are most easily derived if both the ambient medium and the disturbances are assumed to be spherically symmetric (plasma properties are then functions only of the time t and heliocentric distance r). *Parker* [1961, 1963] obtained spherical shock wave solutions of the adiabatic fluid equations (neglecting magnetic forces and solar gravity) by similarity techniques that assume basic dependence on the parameter $\eta = tr^{-\lambda}$. Any feature of these solutions that is at position r_0 at time t_0 moves with time as $r = r_0 (t/t_0)^{1/\lambda}$. The solutions are connected to the ambient medium by assuming a *strong* shock at the leading edge of the disturbances.

Figure 6 shows the density versus position (normalized to the shock location) for two of Parker's shock waves, with a ratio of specific heats $\gamma = 5/3$ and an ambient

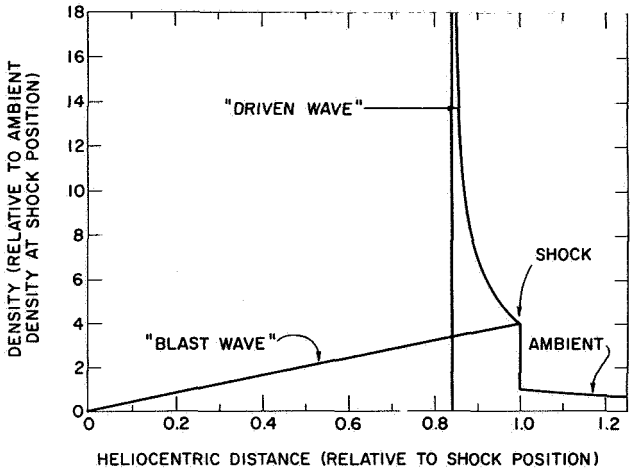

Figure 6. *Similarity solutions for the propagation of spherically symmetric shock waves in the solar wind. The "driven wave" has an energy increasing linearly with time, while the "blast wave" has a constant energy [adapted from Parker, 1961].*

density proportional to r^{-2}. The density change by a factor of 4 at the shock location indicates the assumption of infinite shock strength. The solution labeled *driven wave* corresponds to $\lambda = 1$; the density rises monotonically behind the shock with a singularity as $r \to 0.84$, the position of the vertical line on figure 6. This wave moves with constant speed, and can be shown to have an energy increasing linearly with time. It represents the wave pushed (or driven) ahead of a steadily expanding "piston" (located at the singularity). The solution labeled *blast wave* corresponds to $\lambda = 3/2$; the density falls monotonically behind the shock. This wave moves with steadily decreasing speed, and can be shown to have constant energy. It represents the wave produced by an explosion at $r = 0$, $t = 0$, with no further addition of energy thereafter. This class of "blast wave" solutions (approached by disturbances with energy input occurring over a time short compared to the transit time to a position of interest) has an interesting and useful characteristic; the properties of the wave (e.g., shock speed, transit time to a given radius) depend only on the total energy of the disturbance. The classification of solar wind disturbances as "driven" or "blast" waves will prove useful in the next section. Physically, the driven wave can be thought of as a disturbance whose properties are determined by the nature of the initiating signal at the sun, while the blast wave can be thought of as a disturbance whose properties are determined by interaction with the ambient medium.

Extensions of Parker's basic similarity solutions have been carried out by *Simon and Axford* [1966], *Lee and Balwanz* [1968], *Lee and Chen* [1968], and *Lee et al.*, [1970]. *Korobeinikov* [1969] has derived similarity solutions in which the assumption of infinite shock strength is somewhat relaxed, these solutions being valid to first order in the ratio of the ambient solar wind speed to the shock speed. However, all of these similarity theories of interplanetary shock waves basically apply to strong shocks. Observations (to be discussed in the next section) reveal that most interplanetary shocks are of intermediate strength. The applicability of the similarity solutions to solar wind conditions is therefore questionable.

This difficulty can be overcome by numerical integration of the fluid equations for shocks of arbitrary strength. *Hundhausen and Gentry* [1969*a*, 1969*b*] thus obtained spherical wave solutions of the adiabatic fluid equations (again neglecting magnetic forces, but including solar gravity). Figure 7 shows the density versus

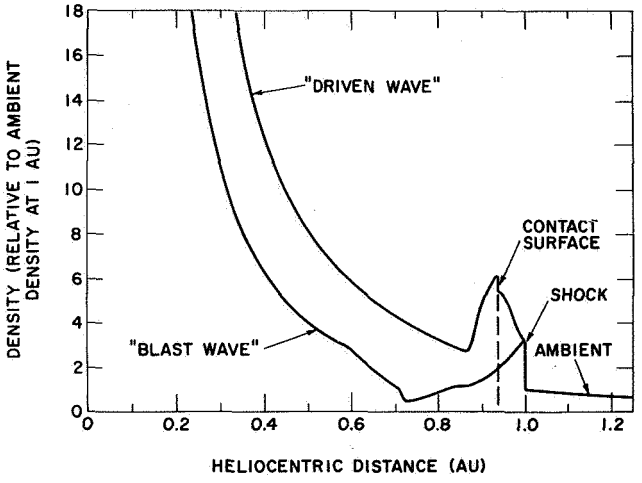

Figure 7. *Numerical solutions for the propagation of spherically symmetric shock waves in the solar wind. The "driven wave" and "blast wave" cases correspond to the same basic definitions used in figure 6 [adapted from Hundhausen and Gentry, 1969a].*

heliocentric position (in AU) for two of these shock waves, with a ratio of specific heats $\gamma = 5/3$ and an ambient adiabatic solar wind with a flow speed of 400 km sec^{-1} and a density of 12 protons cm^{-3} at 1 AU. The density change of less than a factor of 4 at the shock location indicates the finite strength of the shock. The solution labeled *driven wave* shows a monotonic density rise behind the shock until a contact surface, separating the compressed ambient solar wind from the gas ejected in the initial disturbance at $t = 0$, is reached. This interface requires special treatment in the numerical integrations, and its properties are only qualitatively

indicated in figure 7. However, there is no density singularity as found at the "piston" interface in the similarity solutions (the latter appears to be due to the assumption of zero temperature in the similarity theory). The wave moves with nearly constant speed, and has an energy increasing linearly with time. It is thus analogous to the driven wave of similarity theory, representing a wave pushed by a continuous output of driver gas from the sun (forming a new steady state, shown in figure 7 for $r < 0.83$ AU). It differs from the similarity solution of figure 6 in that it considers the flow at heliocentric distances within the contact surface. The numerical solution labeled *blast wave* in figure 7 shows a monotonic decrease in density for some time after the shock, with an eventual increase to the original ambient profile (approximately proportional to r^{-2}) at $r \approx 0.6$ AU. This wave moves with steadily decreasing speed and has a constant total (including gravitational) energy. It is thus analogous to the blast wave of similarity theory, representing a wave produced by a short-duration explosion at $t = 0$, followed here by a return to ambient conditions. As in similarity theory, the properties of this impulsively generated class of waves depend only on the total energy in the disturbance [*Hundhausen and Gentry, 1969a*]. The numerical blast waves differ from those of similarity theory in that the density rarefaction following the shock does not extend all of the way back to the sun.

Figure 8 shows a more detailed comparison of the density (normalized here to the ambient density at any heliocentric radius) versus heliocentric position (normalized to one at the leading-edge shock) for the driven wave solutions derived numerically by *Hundhausen and Gentry* [1969*b*] and using similarity theory by *Simon and Axford* [1966]. Both solutions shown involve a new steady flow at small heliocentric distances that is faster than the flow near the contact surface separating the ambient and "driver gas." Both solutions thus include a "reverse shock" (at S_2 in the numerical solution and at the innermost S in the similarity solution) within the driver gas, as mentioned in the qualitative discussion of the preceding section. *Hundhausen and Gentry* [1969*b*] demonstrated that this configuration will be observed at a given heliocentric position in interplanetary space only if the initiating solar disturbance persists for more than 10 percent of the transit time of the resulting interplanetary shock wave to that position.

The optical emission from nearly all solar flares comes from an area of less than 10^{-3} of a hemisphere [*Smith and Smith,* 1963, pp. 61–63]. Hence the theoretical models described above, all of which assume spherical symmetry of the flare-associated solar wind disturbance,

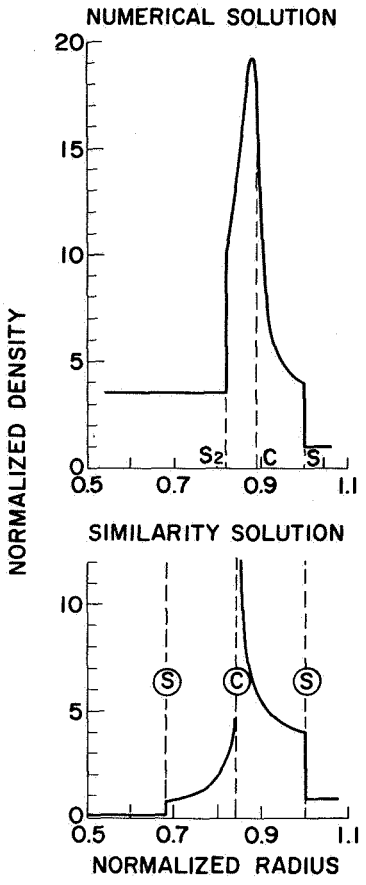

Figure 8. *Numerical and similarity solutions showing the existence of a "reverse shock pair" in the solar wind [Hundhausen and Gentry, 1969b].*

can only roughly approximate reality. *De Young and Hundhausen* [1971] have considered a radially moving flare ejecta confined to a thin spherical shell (at $r = 0.1$ AU) within a cone of half-angle θ (with symmetry axis above the flare site). The propagation of this disturbance into a spherically symmetric, adiabatic ambient solar wind is followed by numerical integration of the hydrodynamic equations. As the energy of the disturbance is constant, it is of the blast wave class defined above. Figure 9 shows the shape of the resulting shock front at several times (in hr) after introduction of a flare ejecta with $\theta = 15°$ and an energy of 2.8×10^{30} ergs. The wave slows and expands laterally in propagating to 1 AU; upon arrival at this distance, 67.6 hr after initiation at 0.1 AU, the shock fills a cone with half angle of nearly 60°. The transverse expansion becomes important when the wave is beyond $r \approx 0.4$ AU because interaction with the ambient medium has considerably slowed and weakened the shock; the high pressure produced behind the front can then produce

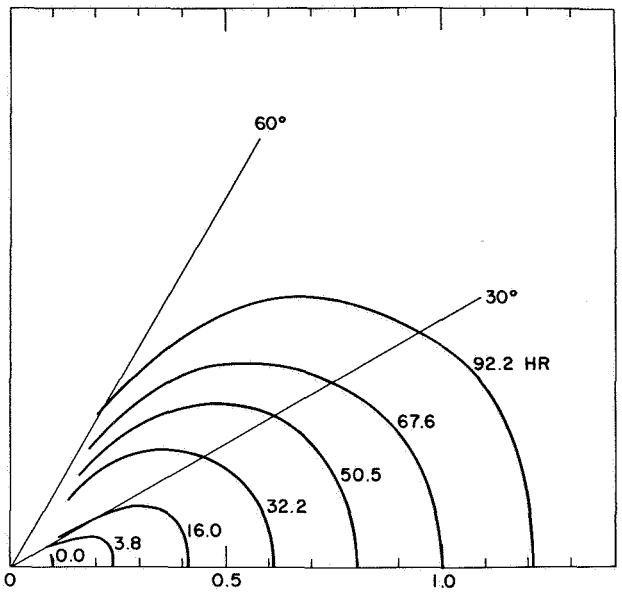

Figure 9. *The shock configuration as a function of time (indicated in hours) produced by a shell of flare ejecta initially confined to a cone with half-angle 15° at a heliocentric distance of 0.1 AU [De Young and Hundhausen, 1971]. On arrival at 1 AU, the disturbance has expanded laterally to fill a cone with half angle of ~60°.*

lateral expansion at a significant fraction of the shock propagation speed.

Figure 10 shows the shapes of the shock fronts (on reaching 1 AU) produced by flare ejecta of the same energy but subtending different half angles when introduced at $r = 0.1$ AU. For $\theta < 15°$, the shock shapes are almost identical; the shock is roughly spherical with radius ~0.5 AU, but centered at 0.5 AU. Thus, for small initial angles, the nonspherical blast waves display an extension of the characteristic of spherical blast waves noted above. The shock shape, as well as the shock speed and transit time, depends on the energy of the initial disturbance, not on such details as the initial angular extent. This characteristic again illustrates the dominant role of the interaction with the ambient medium in determining the properties of blast waves.

Steady, High-Speed Streams

Theoretical models of solar wind disturbances produced by steady, high-speed streams are most logically considered in the frame of reference rotating with the sun (as in fig. 4), wherein the flow is steady although not spherically symmetric (in this sense, the system is at an opposite extreme from the transient, spherical models described earlier). Viewed in this frame, the interaction of a slow ambient solar wind with the high-speed stream is the deflection of a nonuniform, supersonic flow by an impenetrable, curved surface.

No thorough quantitative treatment of this interaction has yet been published. The most pertinent theoretical work in the literature treats corotating, *linear* perturbations of a uniform ambient flow [*Carovillano and Siscoe,* 1969; *Siscoe and Finley,* 1970]. Figure 11 shows the perturbation of the density ρ, the radial velocity component V_r, and the azimuthal velocity component V_ϕ produced at 1 AU by the introduction of a localized, radial, high-speed stream on a source surface at $r = 0.1$ AU [*Carovillano and Siscoe,* 1969]. The abscissa is in units of time for a stationary observer, or, equivalently, the azimuthal angle within the steady structure in the rotating frame (fig. 4). The interaction of the ambient solar wind with the high speed stream has

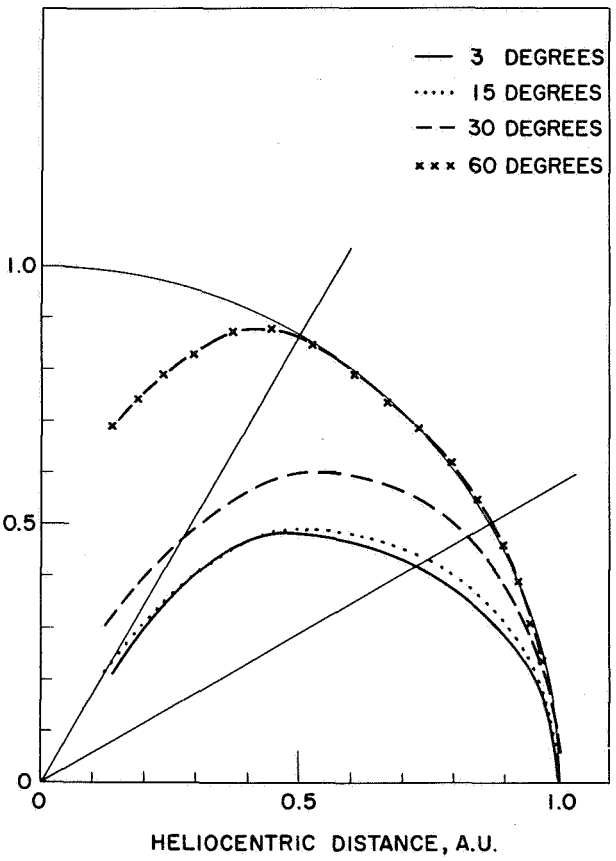

Figure 10. *The interplanetary shock configurations produced by flare ejecta that were initially confined to cones with different half-angles θ at 0.1 AU. For $\theta \lesssim 15°$, the initial half angle has little influence on the configuration near 1 AU [De Young and Hundhausen, 1971].*

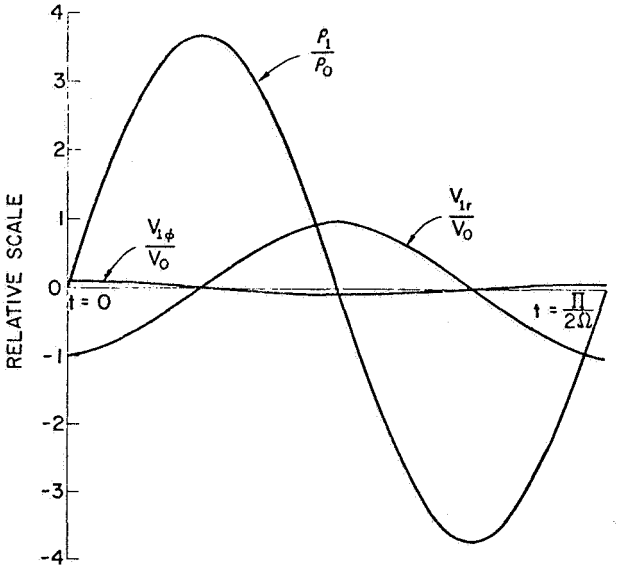

Figure 11. *The linear perturbations in the density ρ, radial velocity component v_r, and azimuthal velocity component v_ϕ produced at 1 AU by a steady high-speed stream, rotating with the sun, introduced at 0.1 AU. The abscissa is the time in a stationary frame of reference rotating with the sun (as in figure 4) [Carovillano and Siscoe, 1969].*

produced the expected density compression and rarefaction in the leading and trailing halves of the disturbance, as well as a small azimuthal velocity component. The nonlinear steepening of the leading edge of the density compression would be expected to ultimately produce a shock. *Mori* [1970] has discussed this process and estimated the heliocentric position of shock formation as a function of the difference in speeds of the ambient solar wind and high-speed stream. This treatment involves several drastic simplifying assumptions (e.g., one-dimensional flow) and does not consider momentum exchange implicit in the interaction of the streams. Its applicability to the actual phenomenon is thus questionable.

Possible Effects of Heat Conduction on Solar Wind Disturbances

For the sake of tractability, all the theoretical models described above have assumed an adiabatic flow of plasma. However, it is expected that the interplanetary plasma is a highly efficient heat conductor. *Parker* [1963] pointed out that the "thermal equilibration time" in the hot plasma behind an interplanetary shock is of the order of 10^4 sec, much shorter than the expected transit time of a flare-produced shock wave to 1 AU. This implies that the flow behind the shock would be more nearly isothermal than adiabatic. *Hundhausen and Montgomery* [1971] have extended this analysis to more general solar wind conditions, arguing that a nearly steady balance will exist between heat conduction and any solar wind heating mechanism persisting on a time scale longer than $\sim 4 \times 10^4$ sec. In fact, the heat conductivity of interplanetary electrons is so large that only a small electron temperature gradient is required to dissipate the energy released at a typical interplanetary shock or in the typical interaction of slow and fast solar wind streams. Heat conduction must then prevent any large rise in electron temperatures associated with such disturbances and ultimately affect their large-scale structure. In the case of flare-produced shock waves, heat conduction should broaden the entire wave structure [*Parker*, 1963]. In the case of steady streams, heat conduction might even prevent the formation of shocks in front of high-speed streams.

OBSERVATIONS OF SOLAR WIND DISTURBANCES

Many detailed observations of interplanetary shock waves have been reported in the literature and discussed in the reviews by *Wilcox* [1969] and *Hundhausen* [1970*a*, *b*]. The emphasis here will be on placing the observations within the context of the large-scale structure of solar wind disturbances. After some illustration of the difficulties encountered in relation specific interplanetary shock waves to specific solar activity, some pertinent observations are presented (with reference to the reviews already mentioned for most details) and a general description of a typical flare-associated disturbance synthesized from the various pieces of observational evidence.

The Relationship Between Interplanetary Shock Waves and Solar Activity

The study of solar-terrestrial relationships was pursued long before any direct observations of the intervening medium were possible. Statistical correlations of solar and geomagnetic activity provided both some general cause-and-effect relationships and some specific inferences regarding the geometry of interplanetary disturbances. Unfortunately, interpretation of such indirect studies was not always unambiguous. To cite only a recent example, *Bell* [1961] has found that over half of the major flares (basically important 2+ or greater) from the years 1937 through 1959 produced a geomagnetic storm within three days, while *Ballif and Jones* [1969] have advocated geomagnetic storms "can be accounted for entirely by the effects of interplanetary streams," with no consideration of emissions from individual flares being necessary. One might conclude that the heritage of the presatellite era is a mixture of wisdom and confusion.

Direct interplanetary observations of shock waves and

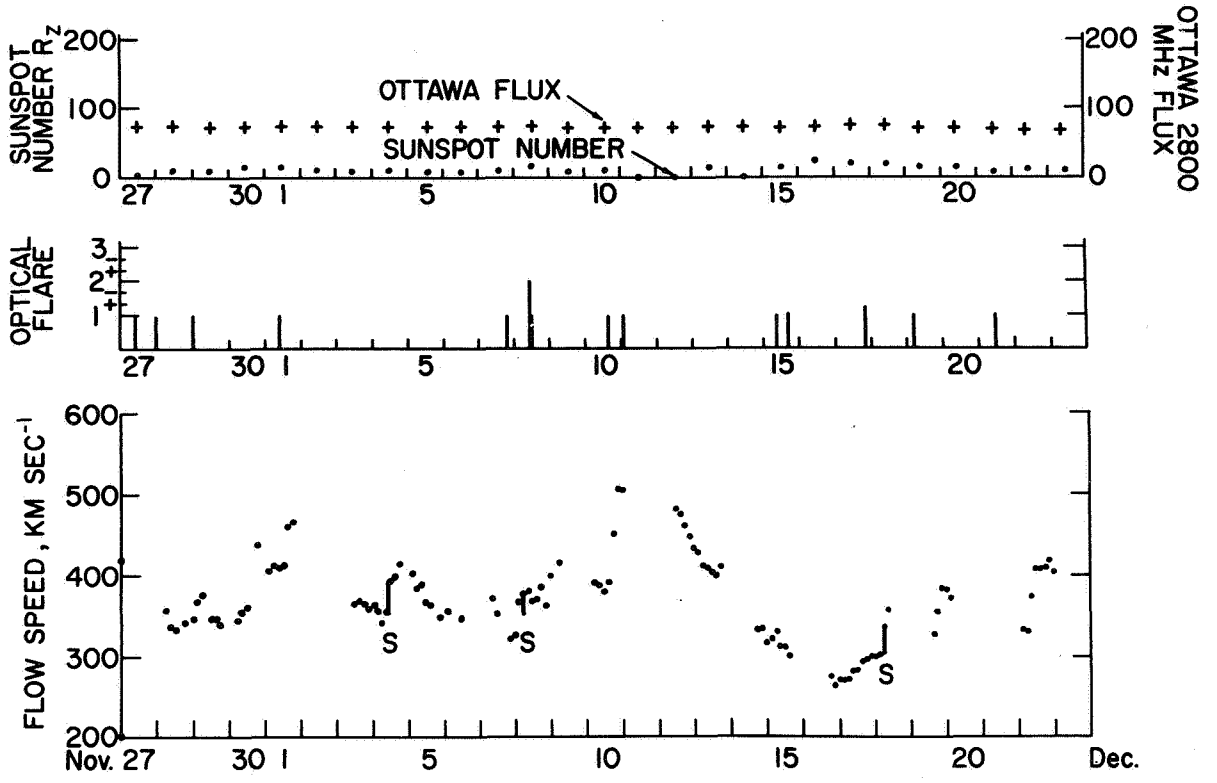

Figure 12. *A summary of solar and interplanetary observations made during the 27-day solar rotation period 27 November to 24 December 1965. Zurich sunspot number, Ottawa 2800 MHz radio flux, optical flare observations (with importance rating denoted by the length of the vertical line), and the 3 averages of the solar wind speed observed on Vela 3 satellites are shown as functions of time. Interplanetary shock waves detected in the Vela 3 observations are denoted by the vertical bars (indicating the observed change in flow speed) and the letter S along the flow speed curve.*

correlations of these observations with indices of solar and geomagnetic activity have added to this heritage. Some observed shock waves can be reasonably attributed to large solar flares, others can be attributed only to small flares, and some have no reasonable flare associations. A few large flares appear to produce no interplanetary shock waves. The relationship between solar activity and solar wind disturbances is still, in fact, imperfectly understood. A few illustrations of specific difficulties are in order.

Figure 12 summarizes solar and interplanetary observations from a 27-day solar rotation period in late 1965. Daily values of the Zurich sunspot number R_Z and the Ottawa index of 2800-MHz solar radio flux, taken from *Solar-Geophysical Data* [1967], are shown in the first frame. Solar flares listed in the same compilation are shown in the second frame by vertical lines whose lengths denote optical importance. Three-hour averages of the solar wind speed observed by Vela 3 spacecraft [*Bame et al.*, 1971] are shown in the lowest frame; interplanetary shocks discernible in the Vela data are indicated by a vertical bar, indicating the observed change in flow speed, and the letter *S* along the flow speed versus time curve.

The low level of solar activity during this period can be judged from the low sunspot numbers and radio fluxes. Only 14 solar flares of importance 1 or greater, including only one flare rated at importance 2 by a single station, were reported during these 27 days. The Vela solar wind observations detected three small interplanetary shock waves; other shocks might have gone undetected during gaps in spacecraft telemetry. None of the three observed shock waves appears to be recurrent [*Hundhausen et al.*, 1970] or associated with a high speed stream of the nature described by *Neugebauer and Snyder* [1966]. Reasonable flare associations can be proposed for the 3 December and 18 December shocks, but these associations must of necessity involve flares of importance 1

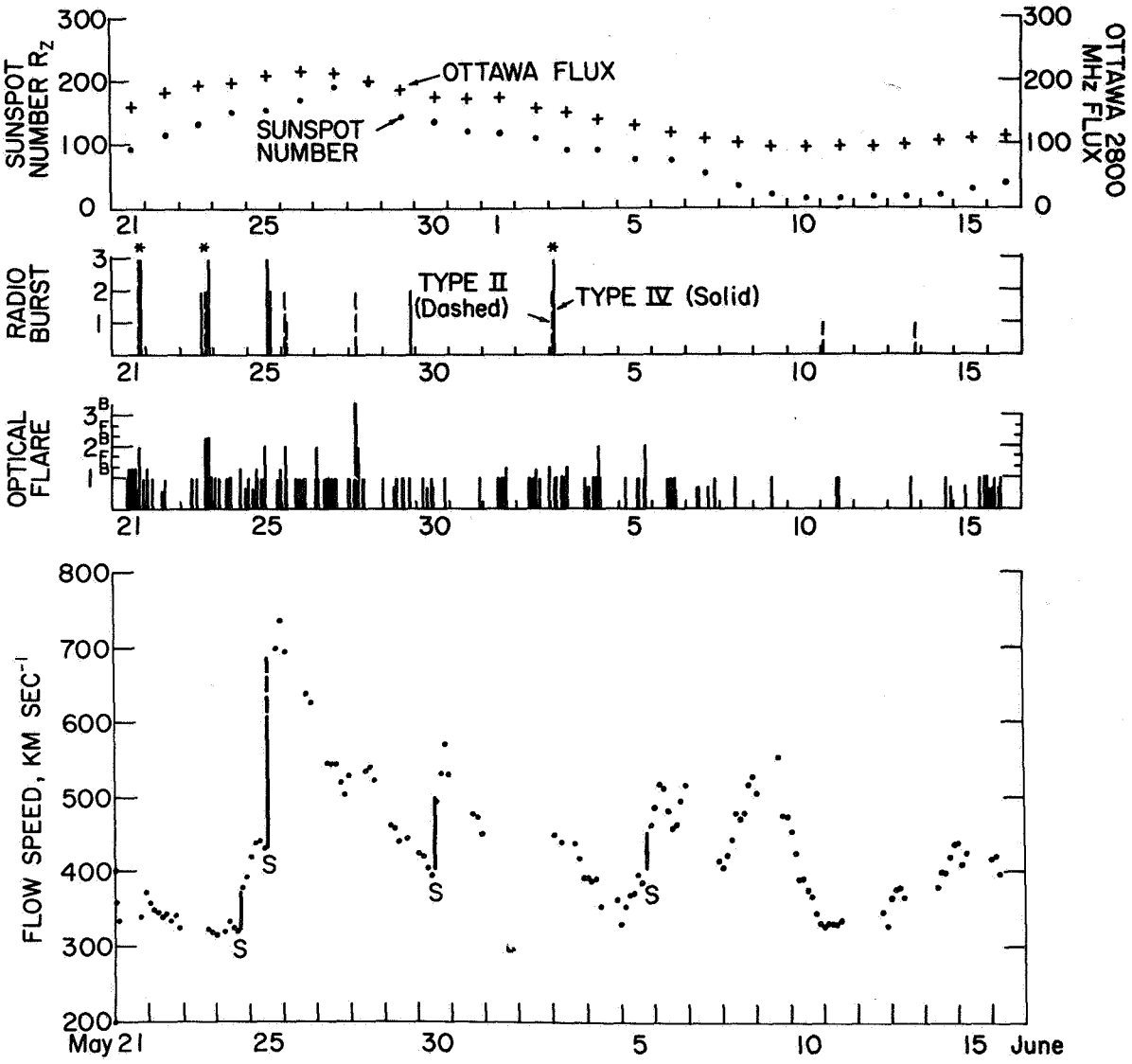

Figure 13. *A summary of solar and interplanetary observations made during the 27-day solar rotation period 21 May to 17 June 1967. Type II and type IV radio bursts, indicated by dashed and solid lines (whose lengths again denote importance), respectively, have been added to the data shown in figure 12. Simultaneous type II and type IV bursts are emphasized by asterisks above the events.*

(i.e., flares with optical emission from a rather small area). Even during this time of low solar activity, there is no unambigous relationship between the observed solar activity and interplanetary disturbances.

Figure 13 summarizes solar and interplanetary observations from a solar rotation in mid-1967. In addition to the information given in the previous example, figure 13 includes type II and type IV radio bursts from the compilations in *Solar-Geophysical Data* [1967] and the *Quarterly Bulletin on Solar Activity* [1967]. The bursts are shown by vertical lines, dashed for type II, solid for type IV, whose lengths indicate importance on the scale (based on maximum intensity) used in the above sources.

Solar activity was at a much higher level during this rotation than during the previous example, as attested by the higher sunspot numbers and 2800-MHz radio fluxes. This difference is manifested in the reporting of 147 importance 1 flares, 12 importance 2 flares, and 2

importance 3 flares during the May-June 1967 solar rotation. It may then be somewhat surprising to find that Vela 3 and Vela 4 satellites detected only four interplanetary shock waves during this rotation. None of the solar wind disturbances related to these shocks appears to be recurrent. Any attempt at flare associations encounters a problem completely different from the paucity of flares in the previous example; in the present example there are many more flares (even many more major flares) than observed interplanetary shock waves.

Consideration of the radio burst data might be expected to help in clarifying flare associations, as type II and type IV bursts are generally attributed to flare-related coronal processes and have been statistically related to geomagnetic storms. In particular, the occurrence of "a combined type II-type IV burst, which indicates a shock front moving ahead of a plasma cloud through the solar corona" [*Kundu*, 1965, p. 553], has a very high correlation with geomagnetic activity. Three such combinations, hereafter referred to as II-IV radio burst pairs, occurred during the solar rotation under discussion and are indicated on figure 13 by asterisks above the vertical lines denoting the bursts. Each burst pair can be associated with a solar flare and was followed within three days by an interplanetary shock wave observation at 1 AU. Consideration of the radio burst data thus leads to an entirely reasonable set of flare–radio burst–interplanetary shock associations: an importance 2N flare and a II-IV burst pair on 21 May with the interplanetary shock observed on 24 May, one of several importance 2B flares and a II-IV burst pair on 23 May with the interplanetary shock observed on 25 May; and an importance 1 flare and a II-IV burst pair on 3 June with the interplanetary shock observed on 5 June. It is curious that the last of these associations favors an importance 1 flare over two later importance 2 flares as the origin of the June 5 shock. The only remaining interplanetary shock from this rotation period, that of 30 May, can be assigned a reasonable association with an importance 3 flare and simultaneous type II burst (but with no reported type IV burst) on 28 May. Thus use of a combination of optical flare and radio burst data brings some order out of the original chaos, leading to a highly plausible association for each observed interplanetary shock wave. The conclusion remains, as stated earlier, that some large solar flares (importance 2 or greater) do not produce interplanetary shock waves.

Further evidence for the usefulness of combined type II-type IV radio bursts in assigning flare associations, as well as a devastating proof that all is not simple, can be found in observations from two successive solar rotations at a level of solar activity intermediate between the examples already discussed. Figure 14 shows sunspot number, 2800-MHz radio flux, type II and type IV radio bursts, optical flares, and solar wind speeds for a solar rotation in February 1967. Two interplanetary shock waves were observed by Vela 3 satellites, each following an importance 2 or 3 flare and a simultaneous II-IV burst pair by the canonical two to three days. The pattern of successful associations of such events was broken on 22 February when a new active region, associated with the plage area McMath 8704, appeared on the east limb of the sun. Figure 15 extends the solar and interplanetary observations through the transit of this active region across the visible solar hemisphere. Many flares, including five with importance ratings as high as 2, were observed within the active region. Four II-IV radio burst pairs, presumably related to some of these flares, were reported during the transit of McMath 8704. Yet no interplanetary shock waves were detected by the Vela 3 satellites; in fact, no major solar wind disturbance is revealed in the flow speed data of figures 14 and 15 for the entire period of transit. Despite a high level of optical flare and radio burst activity, despite the high general level of activity evidenced by the sunspot numbers and 2800-MHz radio fluxes, this active region produced very little perturbation of the solar wind at 1 AU. The interval from 22 February to 16 March is, in fact, the most extended interval of undisturbed solar wind (characterized by low and relatively steady flow speeds) observed by the Vela 3 satellites between July 1965 and June 1967.

Despite the ample demonstration afforded by the above examples of our imperfect understanding of the relationship between solar activity and interplanetary disturbances, some hope can be salvaged from the frequent correlations between the combination type II-typeIV radio bursts and observed interplanetary shock waves. For example, during the first 6 months of 1967, 17 II-IV burst pairs were reported. Nine of the burst pairs were followed within one to three days by an interplanetary shock wave discernible in Vela 3 data; eight of these bursts could be related to simultaneous solar flares that occurred at solar longitudes within 51° of central meridian. Eight of the 17 reported burst pairs were not followed by observed interplanetary shock waves; of these, 3 could be related to flares at solar longitudes greater than 51° from central meridian, while 4 could be related to flares in the infamous McMath 8704 discussed above. Thus 60 percent of the II-IV radio burst pairs related to flares within ~ 50° of central meridian, a restriction similar to those derived in some indirect studies such as that by *Akasofu and Yoshida*

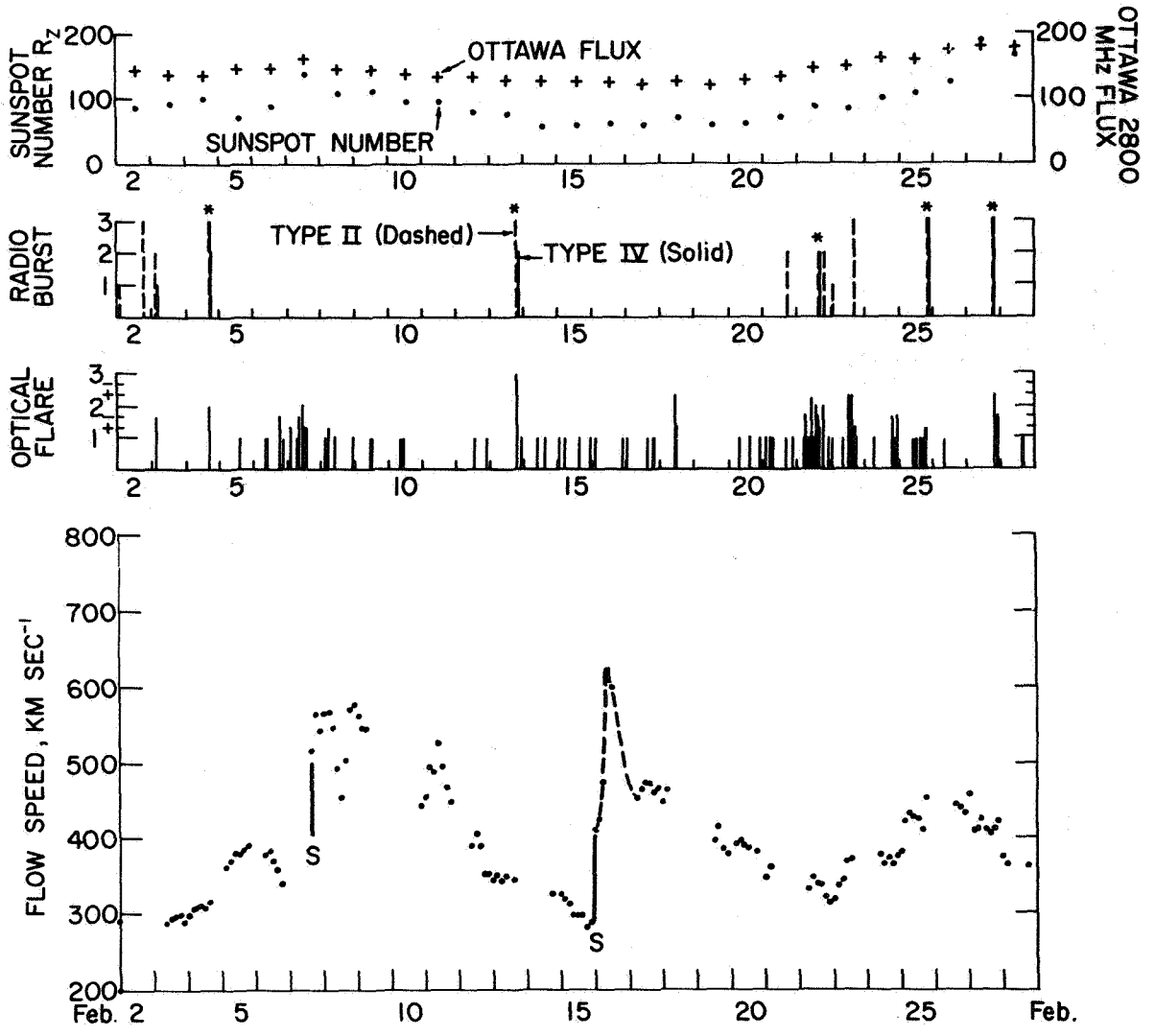

Figure 14. *A summary of solar and interplanetary observations made during the 27-day solar rotation period 2 February to 1 March 1967.*

[1967], were followed by an observed interplanetary shock wave. Particular active regions, such as McMath 8704, however, can be completely anomalous. A test on the necessity of II-IV burst pairs for the occurrence of interplanetary shock waves (the discussion above tests sufficiency) yields a similar result. During the first half of 1967, 9 of the 15 interplanetary shock waves detected by Vela 3 satellites were preceded (within three days) by reported II-IV radio burst pairs (note that daily gaps do exist in solar spectral observations). This latter test works much less well for the solar rotation from late 1965, discussed as the first example above. In fact, *Hundhausen* [1970*b*] and *Hundhausen et al.* [1970] list 7 shock observations from the last half of 1965, while not one II-IV burst pair is reported from these 6 months. However, the shock waves observed in late 1965 were found to be an order of magnitude less energetic than those observed in early 1967; if radio emission were similarly less energetic in 1965, bursts might have occurred but fallen below the threshold of observation. The correlation of radio burst and solar wind observations clearly deserves further and more detailed study.

Local Properties of Interplanetary Shocks

The properties of 27 individual interplanetary shocks observed on various satellites between October 1962 and February 1969 are tabulated in the review by *Hundhausen* [1970*b*]. Table 1 summarizes the dynamic properties of the "typical" shock drawn from this sample. Relevant to the present discussion are the

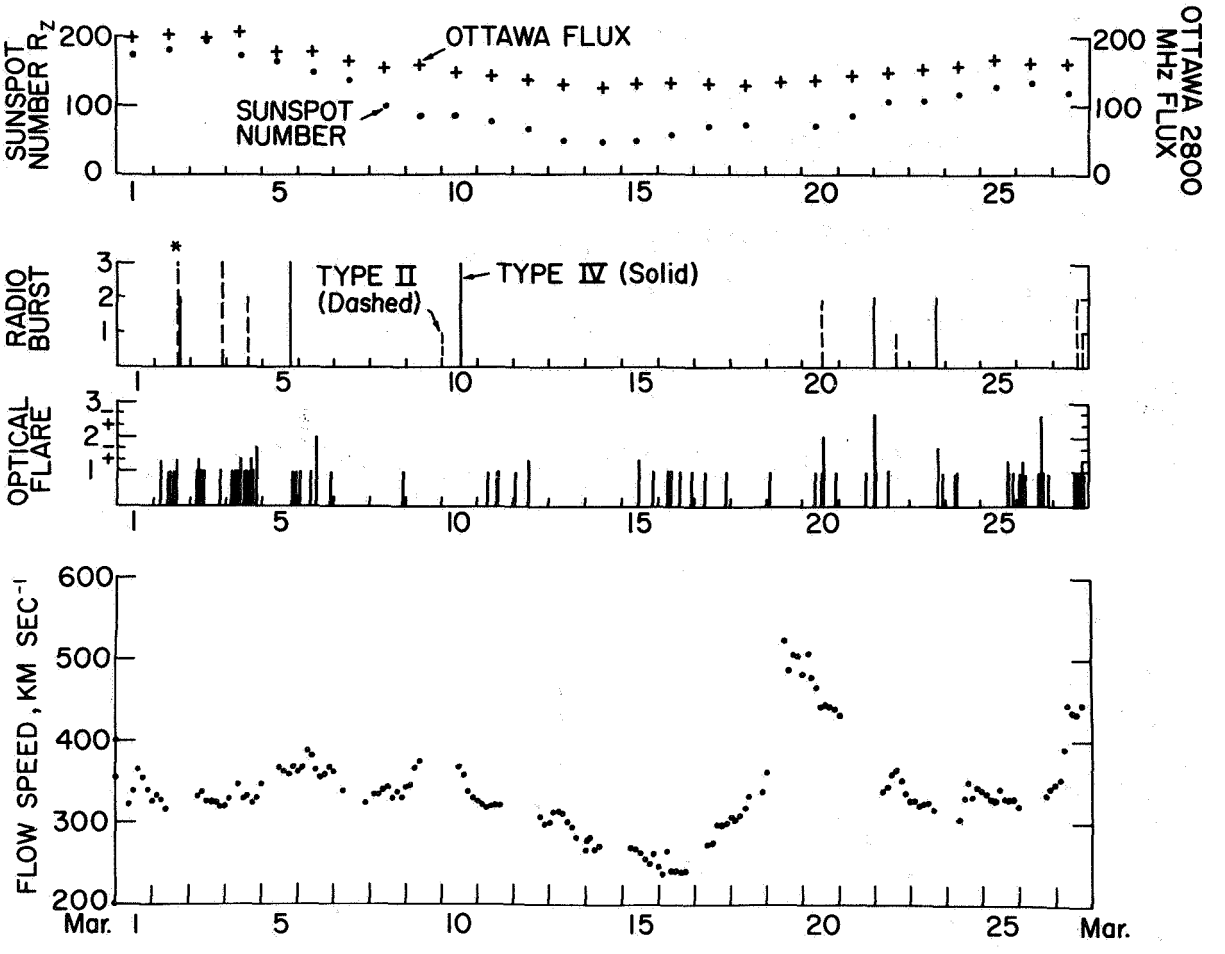

Figure 15. *A summary of solar and interplanetary observations made during the 27-day solar rotation period 1 March to 28 March 1967.*

following conclusions:

1. Interplanetary shocks are not strong (of high Mach number) but rather of intermediate strength. Two implications follow from this conclusion. First, theoretical models that assume strong interplanetary shocks must be applied to solar wind disturbances with some caution. Second, the motion of a shock through interplanetary space is largely the result of the general outward flow of the solar wind plasma rather than the propagation of the shock relative to the plasma. The geometric configuration of the shock wave will then be *strongly* influenced by irregularities in the plasma flow. In particular, the large-scale shock shape can be greatly distorted from the idealized configurations of figures 2 and 5 by a spatial structure of the *ambient* solar wind.
2. Both the similarity and numerical models of interplanetary shock propagation yield relationships between transit time to a given heliocentric distance and the energy in the shock wave, valid for "blast-wave" or impulsively generated disturbances. These relationships have been used to infer shock wave

Table 1. *Dynamical properties of the typical interplanetary shock observed near 1 AU (based on the tabulation in [Hundhausen, 1970b])*

Flow speed of preshock plasma	390 km sec^{-1}
Flow speed of postshock plasma	470 km sec^{-1}
Shock propagation speed relative to stationary observer	500 km sec^{-1}
Shock propagation speed relative to ambient solar wind	110 km sec^{-1}
Mach number (sonic or Alfvén)	2 to 3
Transit time from the sun	55 hr

energies from transit times by *Dryer and Jones* [1968], *Hundhausen and Gentry* [1969*a*], *Korobeinikov* [1969], and *De Young and Hundhausen* [1971]. The 55-hr average transit time given in table 1 leads to an energy estimate of a few times 10^{32} ergs from similarity theory, or of a few times 10^{31} ergs (at 1 AU) from the numerical computations. These estimates assume that the typical interplanetary shock wave is of the blast wave class, and are dependent on both the models and flare associations. A comparison with more directly derived shock wave energies is presented later in this paper.

The local orientations of interplanetary shocks are of special interest as indicators of large-scale shock configurations. A basis for deriving shock orientations from spacecraft observations of the vector magnetic fields, $\mathbf{B}_1$ in the preshock or ambient plasma, and $\mathbf{B}_2$ in the postshock plasma, is the so-called "coplanarity theorem." Application of Maxwell's equations and momentum conservation to a compressive shock front in a medium with isotropic pressure tensor shows [*Colburn and Sonett*, 1966] that the shock normal must lie in the plane defined by $\mathbf{B}_1$ and $\mathbf{B}_2$. *Chao* [1970] has demonstrated that this theorem remains valid in an anisotropic medium if the pressure tensor is symmetric about the magnetic field (as one would expect on the basis of physical symmetry arguments). As $\Delta\mathbf{B} = \mathbf{B}_2 - \mathbf{B}_1$ must lie in the plane of a shock (to satisfy $\nabla \cdot \mathbf{B} = 0$), it follows that the shock normal is parallel to $\Delta\mathbf{B} \times (\mathbf{B}_1 \times \mathbf{B}_2)$. Thus, in principle, observation of the preshock and postshock magnetic fields is sufficient to determine a shock orientation. This technique was applied to actual observations by *Sonett et al.* [1964] and *Ogilvie and Burlaga* [1969]. In practice, however, the coplanarity method does not usually lead to an accurate determination of shock orientation; fluctuations in the fields of the preshock and postshock plasmas and the small change in field direction that occurs at many shocks conspire to produce large uncertainties in the computed normal. *Ogilvie and Burlaga* [1969] were forced to use observations from two spacecraft to derive acceptable normals for several shocks despite the availability of magnetic field observations.

Using both coplanarity and dual-satellite observations *Ogilvie and Burlaga* [1969] derived six shock normals, which gave the first direct statistical evidence regarding shock configurations near 1 AU. These normals clustered about the radial from the sun, with a 20° average deviation therefrom. This distribution is qualitatively consistent with expectations for the shock configuration of figure 2—that is, the flare-produced case. *Taylor* [1969] combined the $\Delta\mathbf{B}$ observed by the IMP 3 magnetometer at 8 "possible shocks" (no unambiguous identification was possible due to the lack of plasma data) having reasonable flare associations with the assumption that the normal was parallel to the ecliptic plane. The resulting shock orientations are shown in figure 16 at a position (on the circle representing 1 AU)

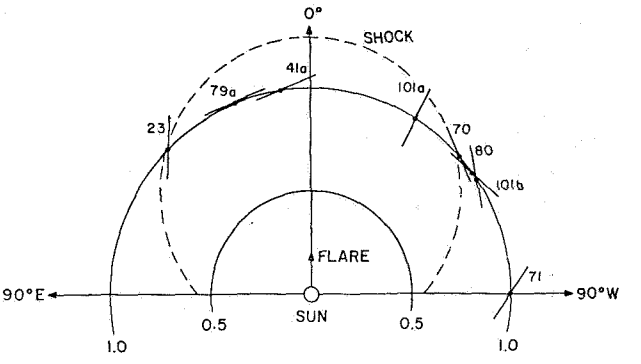

Figure 16. *The orientations of eight shock surfaces inferred from IMP 3 magnetometer data, each plotted at the heliocentric longitude of observation relative to the associated flare [Taylor, 1969].*

corresponding to the solar longitude of each actual observation, relative to the site of the associated flare. All of the shocks except that labeled 101*a* are consistent with shock propagation over a broad front roughly symmetric about the flare site. The dashed line on figure 16 is a circle of radius 0.75 AU centered at 0.5 AU, judged by Taylor to be a reasonable representation of the shock configuration implied by the IMP 3 observations. A similar configuration was proposed by *Hirshberg* [1968] from a statistical study of geomagnetic sudden commencements and solar flares.

Two more complex techniques for derivation of shock normals have been proposed to reduce the uncertainties inherent in the coplanarity method. *Chao* [1970] has used the time delay between observations of a shock at *two different locations* to improve the shock orientations and propagation speeds derived from detailed data obtained at one position. Figure 17 shows five shock normals determined by Chao from Mariner 5 and Pioneer 6 or 7 data. These normals cluster at approximately an average direction about 20° from the radial, with a spread similar to that obtained by *Ogilvie and Burlaga* [1969]. *Lepping and Argentiero* [1970] combine mass and momentum conservation with Maxwell's equations to derive an overdetermined system of equations in the plasma densities, flow speeds, and magnetic field components of the preshock and postshock plasmas. A least-squares fit of these equations to plasma and magnetometer data, accumulated before and after shock

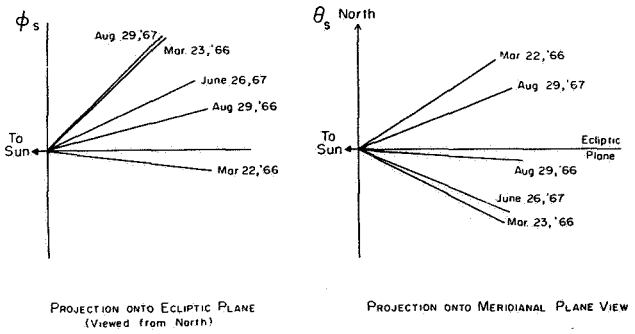

Figure 17. *The orientations of five shock normals derived by Chao [1970]. The angle θ_s is solar ecliptic latitude, while ϕ_s is solar ecliptic longitude.*

passage at a *single* spacecraft, then reduces the effects of fluctuations within the accumulation periods and yields a more accurate shock orientation. This technique has been applied to only a few actual observations.

Characteristics of the Postshock Plasma

The plasma observed after the passage of an interplanetary shock wave is initially the compressed ambient solar wind and ultimately the flare ejecta or high-speed stream responsible for the solar wind disturbance. The properties of these two regimes of postshock plasma are influenced both by the original (near-sun) properties of the ejecta or stream and by the interaction with the ambient solar wind. The shock propagation models described in the preceding section suggest a classification scheme for the dynamical properties of flare-associated disturbances based on the dominance of one or the other of these influences. In the "driven waves," the continual addition of mass, momentum, and energy to the disturbance dominates the dynamics of its propagation and results in a negligible interaction with the ambient plasma. This extreme case is characterized at a given position by continued increases in density and flow speed after the abrupt increases at shock passage. In the "blast waves," the finite mass, momentum, and energy in the disturbance are ultimately less than those in swept-up ambient plasma, so that the interaction with the ambient dominates the dynamics of wave propagation. This extreme case is characterized at a given position by steady decreases in density and flow speed after the abrupt increases at the shock. Although no similar quantitative foundation exists for steady-stream disturbances, a similar classification scheme, based on mass, momentum, and energy fluxes, can be envisioned. The concepts of driven and blast waves will prove useful in organizing observations of the postshock plasma and provide some evidence regarding the duration of energy release in a solar flare. The thermodynamic and chemical characteristics of the ejecta or steady stream would be expected to be retained, as discussed earlier, regardless of the dynamical evolution of the disturbance.

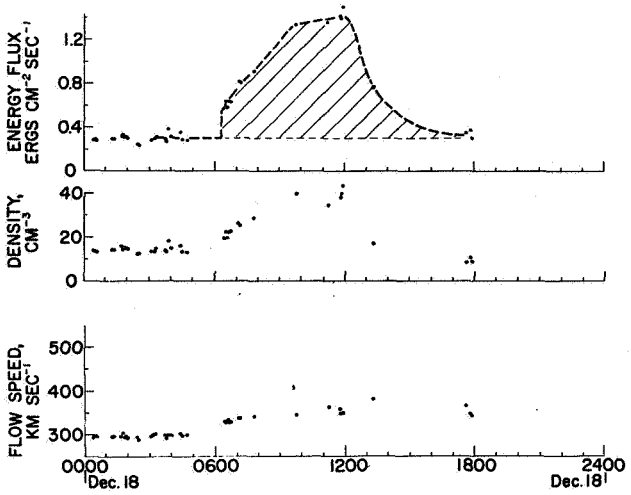

Figure 18. *The solar wind density, flow speed, and kinetic energy flux density observed on 18 December 1965 [Hundhausen et al., 1970].*

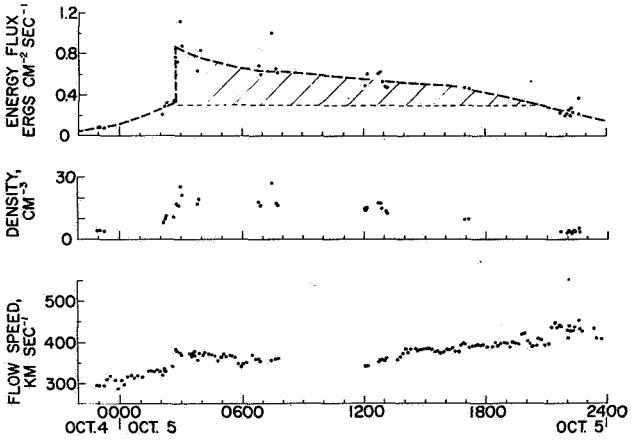

Figure 19. *The solar wind density, flow speed, and kinetic energy flux density observed on 5 October 1965 [Hundhausen et al., 1970].*

Figures 18 and 19 present contrasting examples of solar wind disturbances observed by the Vela 3 satellites [*Hundhausen et al.*, 1970]. The proton density, flow speed, and (for future use) energy flux density are shown as functions of time for 18 December (fig. 18) and 5 October (fig. 19), 1965. The occurrence of a shock during the data gap near 0600 UT on figure 18 can be inferred from a geomagnetic sudden commencement and is confirmed by direct magnetic field observations from the IMP 3 satellite [*Taylor*, 1969]. As both

the density and flow speed continued to rise for some 6 hr after this shock, the disturbance of 18 December qualitatively fit the pattern of postshock plasma variations expected for a driven wave. A shock is clearly indicated in figure 19 by the abrupt rises in density and flow speed just before 0300 UT. As both quantities decreased for some six hours after the shock, the disturbance of 5 October qualitatively fit the pattern of post shock plasma variations expected for a blast wave. The numerical shock propagation models of *Hundhausen and Gentry* [1969*a*, *b*] predict a driven wave-like disturbance profile near 1 AU if energy release near the sun persists for more than ~20 percent of the transit time, a blast wave-like disturbance profile if energy release persists for less than ~8 percent of the transit time, and an intermediate disturbance profile (in which the density rises but the flow speed falls after shock passage) for intermediate durations of energy release. The observation of both driven and blast wave profiles, along with transit times in the range 40 to 60 hr, thus implies that energy release by flares must occur on time scales varying from less than 1 hour to several hours. It has generally been found [*Ogilvie and Burlaga,* 1969; *Hundhausen,* 1970*a, b; Lazarus et al.*, 1970] that the driven wave or intermediate disturbance profiles are most commonly observed near 1 AU.

Despite the general resemblance of the 5 October solar wind disturbance (fig. 19) to a blast wave, the rise in flow speed after 1200 UT is a distinct deviation from the expected pattern. High speed, low-density solar wind was, in fact, observed for several days after this shock. *Hundhausen et al.* [1970] have emphasized that such a persistent stream of high-speed solar wind is observed after most interplanetary shocks (figs. 12 through 14 illustrate this generality) and used a classification scheme for solar wind disturbances based on the rising or falling nature of the postshock energy flux (as shown in figs. 18 and 19). This interpretation of flare-associated disturbances involves a two-stage origin; an enhanced mass and energy injection into the solar wind by the flare, with a duration on the few hour time scale deduced above, followed by a flow of high-speed, low-density solar wind from the general region of the flare for several days thereafter. The persistent high speed stream would be distorted by solar rotation and, despite its flare-related origin, assume some resemblance to the steady-stream configuration of figures 4 and 5.

No observations of a distinct thermodynamic nature of the flare ejecta or steady stream have been reported. Of some interest in this respect are limited observations showing only small changes in the electron temperature at and following an interplanetary shock wave [*Hundhausen,* 1970*d*] and only a minor elevation of the electron temperature in regions where high-speed streams overtake slower solar wind [*Burlaga et al.*, 1971]. *Hundhausen and Montgomery* [1971] have interpreted these results as an effect of heat conduction on solar wind disturbances, as discussed in the preceding section.

Numerous observations do indicate a chemical difference between the compressed ambient solar wind and flare ejecta. The appearance of plasma unusually rich in helium 5 to 12 hr after passage of a shock has been reported by *Gosling et al.* [1967], *Bame et al.* [1968], *Ogilvie et al.* [1968], *Lazarus and Binsack* [1969], *Ogilvie and Wilkerson* [1969], *Hirshberg et al.* [1970], and *Bonetti et al.* [1970]. Figure 20 illustrates this

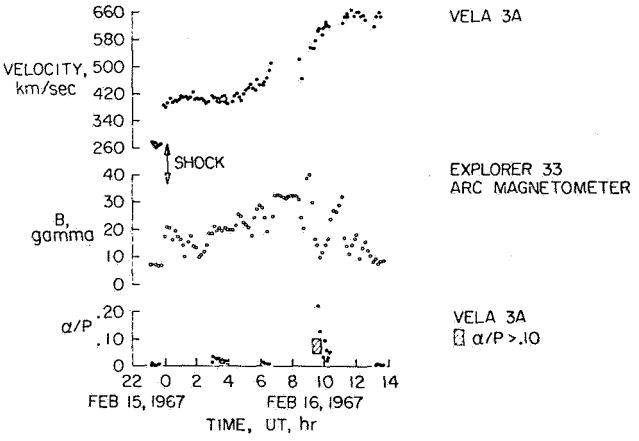

Figure 20. *Solar wind speed, interplanetary magnetic field strength, and the ratio of helium and hydrogen number densities observed on 15-16 February 1967. The shaded area on the lower frame indicates observation of a helium-hydrogen density ratio greater than 0.1 [Hirshberg et al., 1970].*

phenomenon with Vela 3 plasma data and Explorer 33 magnetic field data obtained during the solar wind disturbance of 15-16 February, 1967 [*Hirshberg et al.*, 1970]. The ratios of helium and hydrogen number densities in the plasma observed before the shock and for some 9 hours after the shock were in the range 1 to 2 percent. At 0920 UT, the Explorer 33 magnetometer detected the passage of a tangential discontinuity, discernible in figure 20 as a sudden decrease in the magnitude B of the magnetic field. The plasma following the discontinuity was observed by Vela 3 to have an extremely high helium content, with individual density ratio determinations as high as 22 percent. The helium

content remained above 10 percent for 30 min (indicated by the shaded area on the lowest frame of fig. 20). *Hirshberg et al.* [1970] interpreted the sudden appearance of helium-rich plasma as the arrival of the flare ejecta, separated from the compressed ambient solar wind by the expected tangential discontinuity. The ambient plasma and flare ejecta presumably owe their different chemical compositions either to origins in different regions of a chemically inhomogeneous chromosphere and corona or to their different time histories in expanding from the sun to 1 AU.

One further possible feature of the postshock plasma flow, the reverse shock expected on the basis of the qualitative discussion and quantitative models given earlier, has been the subject of some observational interest. The existence of a small number of reverse shocks has been reported [*Burlaga,* 1970; *Binsack,* 1970], but none has been clearly related to large-scale solar wind disturbances. The apparent rarity of reverse shocks is puzzling, as the high-speed, low-density stream observed to follow most shocks gives precisely the flow condition that should lead to reverse shock formation [*Sonett and Colburn,* 1965; *Hundhausen and Gentry,* 1969*b*; *Hundhausen et al.,* 1970]. Perhaps some energy dissipation mechanism, such as heat conduction, inhibits formation of the shock.

Mass and Energy in Solar Wind Disturbances

The energy in a typical flare-associated solar wind disturbance was estimated at the beginning of this section by using a theoretical relationship between energy and transit time and a mean transit time inferred from flare associations. More direct estimates of the mass as well as the energy can be derived from spacecraft observations at a given heliocentric distance r by integrating the excess of the mass or energy flux (through the sun-centered sphere of radius r) above the ambient value throughout the solar wind disturbance. *Hundhausen et al.* [1970] have applied this technique to Vela 3 and Vela 4 shock wave observations made between August 1965 and July 1967. The flux through the 1 AU sphere was estimated from the observed flux density by assuming that the deviations from ambient conditions were uniform within a π solid angle. This assumption is in reasonable accord with the theoretical shock shapes of *De Young and Hundhausen* [1971], described in the preceding section, or the observational inferences of *Hirshberg* [1968] and *Taylor* [1969], described earlier in this section. The integration over time is illustrated in figures 18 and 19 by the shaded areas under the energy flux density curves. Analysis of 19 nonrecurrent solar wind disturbances led to mass estimates ranging from 5×10^{15} to 1.5×10^{17} gm, with an average of 3×10^{16} gm, and to energy estimates ranging from 5×10^{30} to 2×10^{32} ergs, with an average of 5×10^{31} ergs. The latter value, independent of any theoretical models or specific flare associations, is in excellent agreement with the estimate based on the models of *Hundhausen and Gentry* [1969*a*] and the 55-hr mean transit time to 1 AU given in table 1. The energy released at $1R_\odot$ (corrected from the 1 AU values for the work done against solar gravity) ranges from 1.7×10^{31} to 5×10^{32} ergs, with an average of 1.1×10^{32} ergs. These mass and energy estimates will be discussed in the context of solar flare physical processes in the next section.

Multiple Satellite and Integral Observations

An obvious means of determining the large-scale structure of a solar wind disturbance would be the combination of observations made at several spacecraft separated by distances comparable to the scale size of the disturbance. Unfortunately, only two such multiple satellite observations of an interplanetary shock wave have been reported in the literature. *Lazarus and Binsack* [1969], using Explorer 33 and Pioneer 6 observations, found a significant deviation from spherical symmetry in a shock associated with the 7 July 1966 proton flare. The distortion of the shock wave was attributed to the presence of a spatial structure (related to a magnetic sector) in the ambient solar wind. *Lazarus et al.* [1970] have combined observations from Mariner 5 and Explorer 34, separated by 0.1 AU in heliocentric distance, of an 11 August 1967 solar wind disturbance. A similar disturbance profile, resembling that expected in a driven wave, swept past both spacecraft.

A related technique for the direct observation of the structure of solar wind disturbances involves the Stanford radio propagation experiment, flown on several Pioneer spacecraft, which determines the total electron content along the propagation path between the spacecraft and the earth. The passage of the high-density cloud following an interplanetary shock across this path provides an integrated density measurement from which the gross features of the cloud can be inferred. For example, data obtained from Pioneer 6 on 9 July 1966 indicated the passage of the cloud associated with a shock observed directly by an onboard plasma probe [*Lazarus and Binsack,* 1969]. *Landt and Croft* [1970] have attempted to reconstruct the geometry of the cloud by assuming the presence of two outward moving regions with densities of 140 cm^{-3} and 50 cm^{-3}, values derived from the direct observations. Figure 21 shows the three postshock plasma clouds that could have

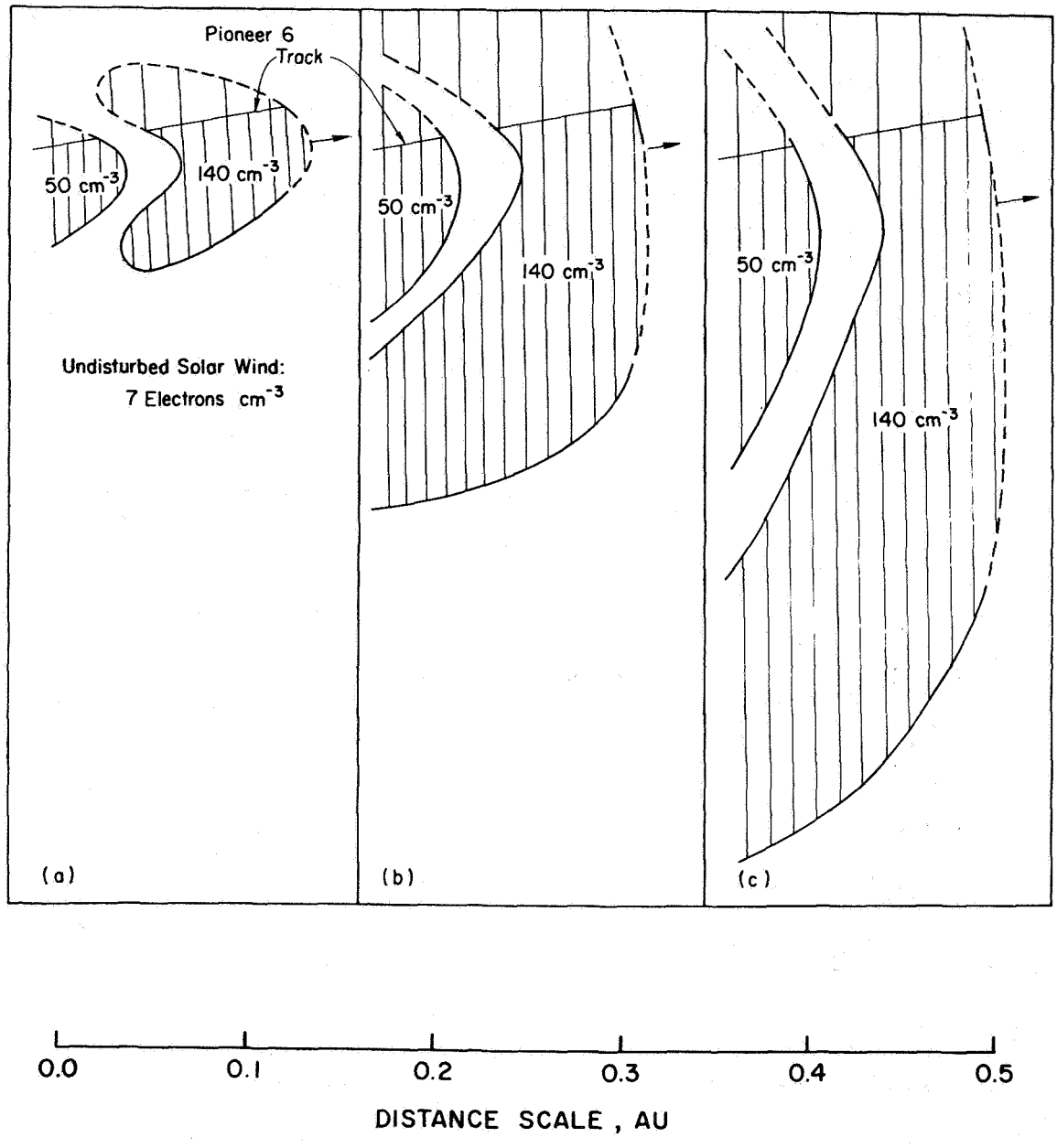

Figure 21. *Three possible plasma cloud shapes inferred from Pioneer 6 radio propagation observations made on 9 July 1966 [Landt and Croft, 1970].*

produced the observed total density signals. Although no objective choice can be made among the three, *Landt and Croft* [1970] favored the disturbance of intermediate size (fig. 21(*b*)). This disturbance has a characteristic size of several tenths of an AU, and is in basic agreement with the other inferences regarding the geometries of solar wind disturbances presented above.

Conclusions

The observations described in this section point to several conclusions regarding the nature and structure of the solar wind disturbances related to interplanetary shock waves. The distributions of observed shock normals are basically consistent with the configuration expected qualitatively (fig. 2) and predicted quantitatively (fig. 10) for a flare-produced disturbance. The ordering in solar longitude of sudden commencements or observed shock fronts relative to the sites of associated flares (fig. 16) and the plasma cloud shape inferred from the integrated electron density (fig. 21) both lead to this

same consistency. None of these pieces of observational evidence is consistent with the expected steady stream-produced shock configuration (fig. 5). In fact, no single directly observed shock has been positively attributed to a steady high speed stream, and most observed recurrent streams [*Neugebauer and Snyder*, 1966; *Hundhausen et al.*, 1970] do not appear to be preceded by shocks. We can only conclude that shocks produced by steady high speed streams are difficult to observe or identify, or are extremely rare. Our present observational knowledge appears to apply to flare-produced solar wind disturbances.

Figure 22 is an attempt to synthesize this knowledge and add some precision to our earlier qualitative

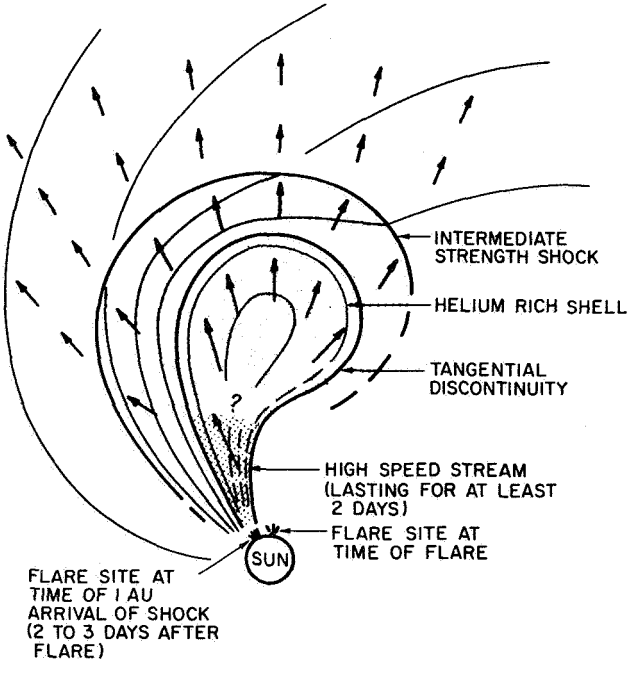

Figure 22. *A sketch, in equatorial cross section, of the observed features of a flare-produced solar wind disturbance (compare with fig 2.).*

description (fig. 2) of a flare-produced disturbance, hereafter considered to be near 1 AU. The shape of the shock at the leading edge of the disturbance is much as previously drawn. The shock is of intermediate strength, propagating through interplanetary space at ~500 km sec^{-1}. The region of compressed ambient solar wind behind the shock is 0.1 to 0.2 AU thick. The tangential discontinuity that separates the compressed ambient plasma from the flare ejecta is sometimes followed by a thin shell (~0.01 AU thick) of helium-rich material. A localized stream of high-speed, low-density solar wind usually follows the flare ejecta: in the two to three days required for the shock wave to reach 1 AU this stream is expected to be distorted into a spiral configuration by solar rotation. Reverse shocks within the flare ejecta or high-speed stream appear only rarely.

Thus many properties of a flare-produced solar wind disturbance are indicated (although in some cases only tentatively) by presently available observations. Many equally interesting properties remain undetermined. For example, there is virtually no observational evidence related to the possible existence of closed field lines within the flare ejecta (as denoted by the question mark on fig. 22). We further note that most of the observations used in this synthesis date from the rising portion of the present solar cycle. These observations do indicate some changes within the cycle—that is, the changes in the energies of disturbances. The large-scale structures of solar wind disturbances might also undergo detailed or gross changes. Clearly, much remains to be learned from future observations.

THE PHYSICS OF SOLAR FLARES

If most interplanetary shock waves are produced by solar flares, as deduced in the preceding section, it is reasonable to attempt to use observations of these waves to infer characteristics of flares. In particular, the estimates of the mass and energy in observed shock waves imply some constraints on the mass and energy release in the flare phenomenon. Before pursuing these implications, a specific warning regarding selection effects is in order.

Both the statistical correlation of solar and geomagnetic activity and the specific relationships between solar and interplanetary observations indicate that not all solar flares, nor even all large solar flares, produce observable interplanetary shock waves. Further evidence for this conclusion has been found in the observation of three transient Faraday rotations of a polarized microwave signal transmitted from Pioneer 6 to earth while the spacecraft moved through occultation by the solar corona [*Levy et al.*, 1969]. *Schatten* [1970] associated each of these events with a specific 1B to 1F flare and interpreted the observed rotation in terms of the expansion and subsequent contraction of a "coronal magnetic bottle" into the microwave transmission path, as illustrated in figure 23. The plasma within the closed field structure or bottle was inferred to be expanding outward at ~200 km sec^{-1} from the delay between the associated flare and the onset of the observed rotation (for the transmission path near $10R_{\odot}$). This expansion is hypothesized to be slowed and ultimately stopped by the tension in the magnetic field lines. After cooling by radiation and heat conduction, the magnetic bottle

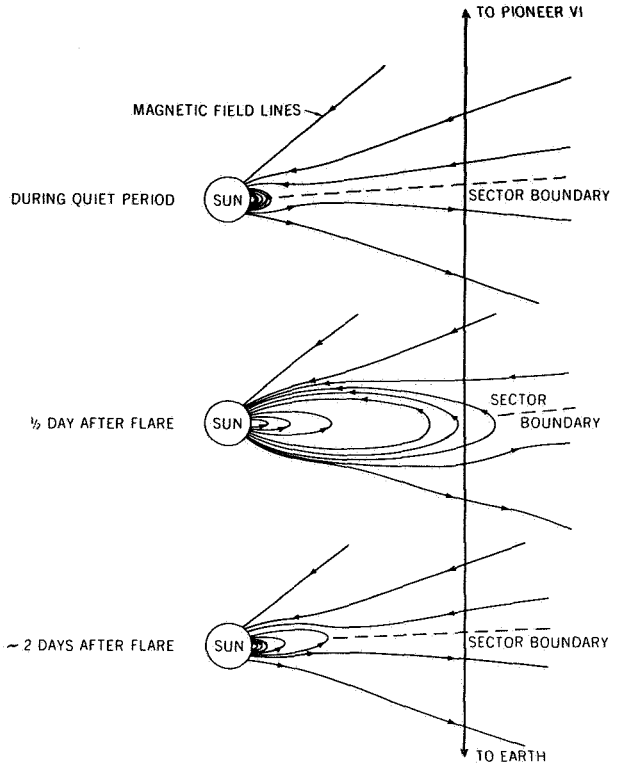

Figure 23. *The coronal magnetic field configurations proposed by Schatten [1970] to account for the transient Faraday rotations of a microwave signal transmitted from Pioneer 6 during occulation by the solar corona.*

presumably contracts to a configuration similar to that of the preshock stage. The energy of the plasma within the structure is estimated to be of the order of 10^{30} ergs, one to two orders of magnitude smaller than that in the interplanetary shocks discussed in the preceding section.

This situation could lead to selection effects; that is, the (unknown) characteristics that allow some flares to produce interplanetary shock waves might not be typical of all flares. In fact, the shock wave mass and energy observations hint that some such selection does take place. Figure 24 shows the estimates of the mass and equivalent energy at $1R_\odot$ for the 19 solar wind disturbances analyzed by *Hundhausen et al.* [1970]. No observation can fall below the dashed line, as an energy of 1.92×10^{15} ergs gm^{-1} has been added to each value derived at 1 AU to account for the work done against solar gravity in transit to the latter distance. Remarkably, all the observations fall in a limited region just above this line, near an equivalent energy per mass of 3 keV per H atom or a temperature of $\sim 10^{7}$°K. This grouping could be interpreted as evidence that all flares produce flare ejecta with essentially the same temperature. However, a completely different interpretation can be proposed. Suppose rather that flares produce ejecta with an effective energy (kinetic plus thermal) per mass distributed about an average that is less than that required for excape to 1 AU against solar gravity, as shown in figure 25. The solar wind disturbances observed at 1 AU would have an equivalent energy (with the gravitational correction back to $1R_\odot$) per mass distributed as indicated by the shaded area under the curve of figure 25, producing an effect similar to that noted in figure 24. In fact, this latter interpretation is in accord with the earlier conclusion that most flares do not produce interplanetary shocks observed at 1 AU. It neglects such important complications as heat conduction or the magnetic forces invoked by Schatten. However, the remarkable ordering of figure 24 in terms of the energy per mass may indicate that solar gravity is a dominant factor in limiting the escape of flare ejecta into interplanetary space.

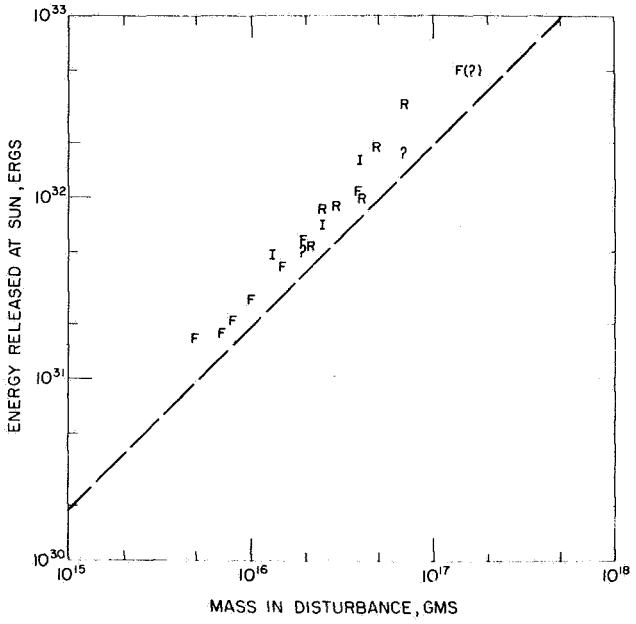

Figure 24. *The mass and equivalent energy at 1 solar radius in 19 interplanetary shock waves analyzed by Hundhausen et al. [1970]. The behavior of the post-shock energy flux is denoted by the symbols R (rising), F (falling), I (intermediate), or ? (undetermined) for each event. The dashed line indicates the gravitational correction added to the energy determined at 1 AU.*

With these possible selection effects in mind, let us finally consider the implications of the interplanetary observations with respect to the mass and energy releases

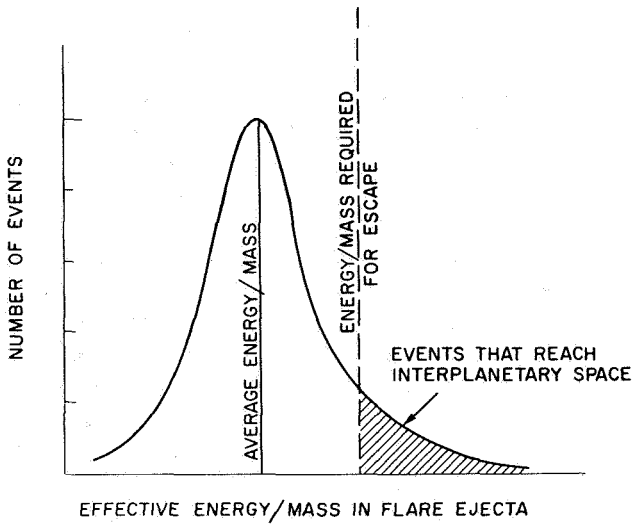

Figure 25. *The effect of solar gravity on flare ejecta whose energy per mass are distributed about an average less than the energy per mass required for escape to 1 AU in the solar gravitational field.*

in solar flares. Of the 19 solar wind disturbances considered by *Hundhausen et al.* [1970], six have highly plausible associations with optical flares accompanied by type II and type IV radio bursts (five of these associations were dicussed among the examples at the beginning of the preceding section). Table 2 summarizes this set of solar-interplanetary associations. Five of these flares were of importance 2 or greater, and could thus be described as large flares. The average optical duration of all six flares was 130 min, comparable to the several hour time scale for energy deposition deduced from interplanetary shock profiles, as well as typical of large flares [*Bruzek*, 1967]. The average mass of the associated solar wind disturbances was 4.5×10^{16} gm, while the average equivalent energy at $1R_\odot$ was 1.6×10^{32} ergs.

The rates of mass and energy addition to the solar wind implied by these mass, energy, and time scale estimates are respectively 6×10^{12} gm sec^{-1} and 2×10^{28} ergs sec^{-1}. The rates of coronal mass and energy loss in the quiet solar wind are 1×10^{12} gm sec^{-1} and 3×10^{27} erg sec^{-1} [*Kuperus*, 1969; *Hundhausen*, 1971]. Thus solar flares, despite having an area of $\lesssim 10^3$ of the total sun, can for a short time supply mass and energy to the solar wind with a total flux greater than that of the entire undisturbed corona.

The optical emission from a large solar flare comes from a volume of $\sim10^{28}$ cm^3 wherein the electron density is $\sim10^{13}$ cm^{-3} [*Bruzek*, 1967]. Thus the mass within the luminous volume is $\sim2\times10^{17}$gm. *Bruzek* [1967] has estimated the mass in visible flare-associated ejections to be $\sim2\times10^{16}$ gm. Thus the mass ejected into interplanetary space, $\sim5\times10^{16}$ gm as deduced above, is roughly equal to that in the visible ejections and an appreciable fraction ($\sim1/4$) of that within the flare region (note that these conclusions differ from those of Bruzek, who estimated a much smaller mass in the interplanetary shock wave.) Mass ejection on this scale must be expected to produce large changes in the chromosphere and corona near the flare site.

Table 2. *Associations of flares and radio bursts with interplanetary shock waves analyzed in Hundhausen et al. [1970]*

Flare				Radio Bursts		Interplanetary Shock Wave			
Date	Imp.	Duration	Position	Type	Duration	Date	Time	Mass(gm)	Energy at Sun (erg)
Feb. 4	2	1641-1902	N11E40	II IV	1708-1728 1705-1846	Feb. 7	1640	4×10^{16}	1.6×10^{32}
Feb. 13	3	1749-2130	N20W10	II IV	1803-1820 1829-2438	Feb. 15	2345	5×10^{16}	1.9×10^{32}
May 3	2B	1537-1926	N25E51	II IV	1548-1603 1603-1650	May 7	0100	3×10^{16}	0.9×10^{32}
May 21	2N	1919-1945	N24E39	II IV	1923-1945 1923-2100	May 24	1730	4×10^{16}	1.1×10^{32}
May 28	3B	0527-0712	N28W33	II	0545-0552	May 30	1430	7×10^{16}	3.3×10^{32}
June 3	1N	0243-0342	N24E14	II IV	0243-0250 0235-0450	June 5	1915	4×10^{16}	1.1×10^{32}

Table 3 compares the average energy at $1R_\odot$ in an interplanetary shock wave, as deduced above, with other energy losses from a large (3+) flare; the tabulation is based on the energy estimates (some valid only to an order of magnitude) given by *Bruzek* [1967], with correction of typographic errors and adoption of the shock wave energy derived herein. All loss processes other than optical emission and the interplanetary shock wave are negligible despite their interest as indicators of physical phenomena. The shock wave appears to carry away about half of the energy released in a flare, with most of the remainder radiated at optical wavelengths. This is in contrast to the energy balance for normal chromospheric and coronal conditions, wherein only about 1 percent of the total energy loss is due to the ambient solar wind flow. The total energy released by the flare must be at least 2×10^{32} ergs. This requires a specific energy release of 2×10^{4} ergs cm^{-3} from the luminous volume of a flare. A comparison with the normal chromospheric thermal energy density of 5 ergs cm^{-3} and the normal coronal energy density of 1 erg cm^{-3} illustrates the magnitude of the problem to be faced in any model of energy storage and release by a solar flare.

Table 3. *Estimated energy releases in a large solar flare*

Process	Energy (ergs)
H-alpha emission	10^{31}
Line emission (including Hα)	5×10^{31}
Continuum emission	8×10^{31}
Total optical emission	10^{32}
Soft X-rays (1 to 20 Å)	2×10^{30}
Radio burst	10^{25}
Energetic protons (E > 10 MeV)	2×10^{31}
Solar cosmic rays (E = 1 to 30 GeV)	3×10^{30}
Visible ejections	10^{31}
Interplanetary shock wave	1.6×10^{32}

ACKNOWLEDGEMENTS

Informative discussions with Drs. S. J. Bame and M. D. Montgomery of the Los Alamos Scientific Laboratory, Dr. J. T. Gosling of the High Altitude Observatory, Dr. L. F. Burlaga of NASA Goddard Space Flight Center, and Prof. A. J. Lazarus of the Massachusetts institute of Technology are acknowledged.

This work was performed under the auspices of the U.S. Atomic Energy Commission.

REFERENCES

Akasofu, S. I.; and Yoshida, S.: The Structure of the Solar Plasma Flow Generated by Solar Flares. *Planet. Space Sci,* Vol. 15, 1967, p. 39.

Ballif, J. R.; and Jones, D. E.: Flares, Forbush Decreases, and Geomagnetic Storms. *J. Geophys. Res.*, Vol. 74, 1969, p. 3499.

Bame, S. J.; Asbridge, J. R.; Hundhausen, A. J.; and Strong, I. B.: Solar Wind and Magnetosheath, Observations During the January 13-14, 1967, Geomagentic Storm. *J. Geophys. Res.,* Vol. 73, 1968, p. 5761.

Bame, S. J.; Asbridge, J. R.; Felthauser, H. E.; Gilbert, H. E.; Hundhausen, A. J.; Smith, D. M.; Strong, I. B.; and Sydoriak, S. J.: A. Compilation of Vela 3 solar wind observations, 1965 to 1967. *Los Alamos Scientific Laboratory LA-4536,* Vol. 1, 1971.

Bell, Barbara: Major Flares and Geomagnetic Activity. *Smiths. Contr. to Astrophys.*, Vol. 5, 1961, p. 69.

Binsack, J. H.: Average Properties of the Solar Wind as Observed by Explorers 33 and 35. *E⊕S. Trans. Amer. Geophys. Union,* Vol. 51, 1970, p. 413.

Bonetti, A.; Moreno, G.; Candidi, M.; Egidi, A.; Formisano, V.; and Pizzella, G.: Observation of Solar Wind Discontinuities from February 24 to February 28, 1969. *Intercorrelated Satellite Observations Related to Solar Events,* edited by V. Manno and D. E. Page, D. Reidel, Dordrecht, 1970, p. 436.

Bruzek, A.: Physics of Solar Flares, the Energy and Mass Problem. *Solar Physics,* edited by J. N. Xanthakis, Interscience, New York, 1967, p. 399.

Bumba, V.; and Obridko, V. N.: "Bartels' Active Longitudes," Sector Boundaries and Flare Activity. *Solar Phys.*, Vol. 6, 1969, p. 104.

Burlaga, L. F.: A Reverse Hydromagnetic Shock in the Wind. *Cosmic Electrodyn.* Vol. 1, 1970, p. 233.

Burlaga, L. F.; Ogilvie, K. W.; Fairfield, D. H.; Montgomery, M. D.; and Bame, S. J.: Energy Transfer at Colliding Streams in the Solar Wind. *Astrophys. J.*, Vol. 164, 1971, p. 137.

Carovillano, R. L.; and Siscoe, G. L.: Corotating Structure in the Solar Wind. *Solar Phys.*, Vol. 8, 1969, p. 401.

Chao, J. K.: Interplanetary Collisionless Shock Waves. MIT center for Space Research preprint CSR TR-70-3, 1970.

Colburn, D. S.; and Sonett, C. P.: Discontinuities in the Solar Wind, *Space Sci. Rev.*, Vol. 5, 1966, p. 439.

DeYoung, D. S.; and Hundhausen, A. J.: Non-spherical Propagation of a Flare-Associated Interplanetary Blast Wave (abstract), *J. Geophys. Res.*, Vol. 76, 1971, p. 2245.

Dryer, M.; and D. L. Jones: Energy Deposition in the Solar Wind by Flare-Generated Shock Waves. *J. Geophys. Res.*, Vol. 73, 1968, p. 4875.

Gold, T.: *Gas Dynamics of Cosmic Clouds,* edited by H. C. van de Hulst and J. M. Burgers, North-Holland Publishing Co., Amsterdam, 1955, p. 103.

Gosling, J. T; Asbridge, J. R.; Bame, S. J.; Hundhausen, A. J.; and Strong, I. B.: Measurements of the Interplanetary Solar Wind During the Large Geomagnetic Storm of April 17-18, 1965. *J. Geophys. Res.*, Vol. 72, 1967, p. 1813.

Hirshberg, J.: The Transport of Flare Plasma from the Sun to the Earth. *Planet. Space Sci.*, Vol. 16, 1968, p. 309.

Hirshberg, J.; Alksne, A.; Colburn, D. S.; Bame, S. J.; and Hundhausen, A. J.: Observation of a Solar Flare Induced Interplanetary Shock and Helium-Enriched Driver Gas. *J. Geophys. Res.*, Vol. 75, 1970 p. 1.

Hundhausen, A. J.: Solar Wind Disturbances Associated with Solar Activity, in *Intercorrelated Satellite Observations Related to Solar Events,* edited by V. Manno and D. E. Page, D. Reidel, Bordrecht, 1970a.

Hundhausen, A. J.: Composition and Dynamics of the Solar Wind Plasma. *Rev. Geophys. Space Phys.*, Vol. 8, 1970*b*, p. 729.

Hundhausen, A. J.: Dynamics of the Outer Solar Atmosphere. Los Alamos Scientific Laboratory Preprint LA-DC-11911 (to be published in the proceedings of the Fourth Summer Institute for Astronomy and Astrophysics, Stony Brook) 1970*c*.

Hundhausen, A. J.: Shock Waves in the Solar Wind. *Particles and Fields in the Magnetosphere,* edited by B. M. McCormac, D. Reidel, Dordrecht, 79, 1970*d*.

Hundhausen, A. J.; and Gentry, R. A.: Numerical Simulation of Flare-Generated Disturbances in the Solar Wind. *J. Geophys. Res.*, Vol. 74, 1969*a*, p. 2908.

Hundhausen, A. J.; and Gentry, R. A.: The Effects of Solar Flare Duration on a Double Shock Pair at 1 AU. *J. Geophys. Res.*, Vol. 74, 1969*b*, p. 6229.

Hundhausen, A. J.; Bame, S. J.; and Montgomery, M. D.: The Large Scale Characteristics of Flare-Associated Solar Wind Disturbances, *J. Geophys. Res.*, Vol. 75, 1970, p. 4631.

Hundhausen, A. J.; and Montgomery, M. D.: Heat Conduction and Nonsteady Phenomena in the Solar Wind. *J. Geophys. Res.* Vol. 76, 1971, p. 2236.

Korobeinikov, V. P.: On the Gas Flow Due to Solar Flares. Solar Phys., Vol. 7, 1969, p. 463.

Kundu, M. R.: *Solar Radio Astronomy.* Interscience, New York, 1965.

Kuperus, M.: The Heating of the Solar Corona. *Space Sci. Rev.*, Vol. 9, 1969, p. 713.

Landt, J. A.; and Croft, T. A.: Shape of a Solar Wind Disturbance on July 9, 1966, Inferred From Radio Signal Delay to Pioneer 6. *J. Geophys. Res.*, Vol. 75, 1970, p. 4623.

Lazarus, A. J.; and Binsack, J. H.: Observations of the Interplanetary Plasma Subsequent to the July 7, 1966 Proton Flare. *Ann. IQSY,* Vol. 3, 1969, p. 378.

Lazarus, A. J.; Ogilvie, K. W.; and Burlaga, L. F.: Interplanetary Shock Observations by Mariner 5 and Explorer 34. MIT Center for Space Research preprint CSR-P-70-36, submitted to *Solar Phys.*, 1970.

Lee, T. S.; and Balwanz, W. W.: Singular Variations Near the Contact Discontinuity in the Theory of Interplanetary Blast Waves. *Solar Phys.* Vol. 4, 1968, p. 240.

Lee, T. S.; and Chen, T.: Hydromagnetic Interplanetary Shock Waves. *Planet. Space Sci.*, Vol. 16, 1968, p. 1483.

Lee, T. S.; Chen, T.; and Balwanz, W. W.: Hydromagnetic Theory for Disturbances Following an Ideal "Solar Thermal Explosion." *E⊕S, Trans. Amer. Geophys. Union,* Vol. 51, 1970, p. 414.

Lepping, R. P.; and Argentiero, P. D.: Improved Shock Normals Obtained From Combined Magnetic and Plasma Data from a Single Spacecraft. NASA Goddard Space Flight Center Preprint X-692-70-276, 1970.

Levy, G. S.; Sato, T.; Seidel, B. L.; Stelzried, C. T.; Ohlson, J. E.; and Rusch, W. V. T.: Pioneer 6: Measurement of Transient Faraday Rotation Phenomena Observed During Solar Occulation. *Science,* Vol. 166, 1969, p. 596.

Mackin, R. J.; and Neugebauer, Marcia: The Solar Wind, Pergamon Press, New York, 1966.

Mori, Y.: Shock Wave Hypothesis on Sudden Commencements of 27-Day Recurrent Geomagnetic Disturbances. *Sci. Rep. of Tohoku Univ., Series 5,* Vol. 19, 1970, p. 135.

Neugebauer, M.; and Snyder, C. W.: Mariner 2 Observations of the Solar Wind, 1, Average Properties. *J. Geophys. Res.*, Vol. 71, 1966, p. 4469.

Ogilvie, K. W.; and Burlaga, L. F.: Hydromagnetic Shocks in the Solar Wind. *Solar Phys.* Vol. 8, 1969, p. 422.

Ogilvie, K. W.; and Wilkerson, T. D.: Helium Abundance in the Solar Wind. *Solar Phys.*, Vol. 8, 1969, p. 435.

Ogilvie, K. W.; Burlaga, L. F.; and Wilkerson, T. D.: Plasma Observations on Explorer 34, *J. Geophys. Res.*, Vol. 73, 1968, p. 6809.

Parker, E. N.: Sudden Expansion of the Corona Following a Large Solar Flare and the Attendant Magnetic Field and Cosmic Ray Effects. *Astrophys. J.*, Vol. 133, 1961, p. 1014.

Parker, E. N.: *Interplanetary Dynamical Processes.* Interscience, New York, 1963.

Parker, E. N.: Theoretical Studies of the Solar Wind Phenomenon. *Space Sci. Rev.*, Vol. 9, 1969, p. 325.

Petschek, H. E.: Reconnection and Annihilation of Magnetic Fields. *The Solar Wind,* edited by R. J. Mackin and M. Neugebauer, Pergamon Press, New York, 1966, p. 221.

Quarterly Bulletin on Solar Activity, Eidgen-Sternwarte, Zurich, 1967.

Schatten, K. H.: Evidence for a Coronal Magnetic Bottle at 10 Solar Radii, *Solar Phys.*, Vol. 12, 1970, p. 484.

Simon, M.; and Axford, W. I.: Shock Waves in the Interplanetary Medium, *Planet. Space Sci.*, Vol. 14, 1966, p. 901.

Siscoe, G. L.; and Finley, L. T.: Solar Wind Structures Determined by Corotating Coronal Inhomogeneities: I. Velocity Driven Perturbations. *J. Geophys. Res.*, Vol. 75, 1970, p. 1817.

Smerd, S. F.: Radio Evidence for the Propagation of Magnetohydrodynamic Waves Along Curved Paths in the Solar Corona. *Proc. Astron. Soc. Australia,* Vol. 1, 1970, p. 305.

Smith, H. J.; and Smith, E. V. P.: *Solar Flares.* Macmillan, New York, 1963. *Solar-Geophysical Data, U. S. Govt. Printing Office,* Washington, D. C., 1965, 1967.

Sonett, C. P.; Colburn, D. S.; Davis, L. Jr.; Smith, E. J.; and Coleman, P. J., Jr.: Evidence for a Collision-Free Magnetohydrodynamic Shock Wave in Interplanetary Space. *Phys. Rev. Lett.*, Vol. 13, 1964, p. 153.

Sonett, C. P.; and Colburn, D. S.: The SI^{+} - SI^{-} Pair and Interplanetary Forward-Reverse Shock Ensembles. *Planet. Space Sci.*, Vol. 13, 1965, p. 675.

Sturrock, P. A.: Solar Flares. *Plasma Astrophysics,* Academic Press, New York, 1967.

Taylor, H. E.: Sudden Commencement Associated Discontinuities in the Interplanetary Magnetic Field Observed by IMP 3. *Solar Phys.*, Vol. 6, 1969, p. 320.

Wilcox, J. M.: Solar Wind Disturbances Associated with Solar Flares. *Solar Flares and Space Research,* edited by Z. Suestka and C. De Jager, North-Holland, Amsterdam, 1969.

DISCUSSION

C. P. Sonett In the case of the reverse shock it was pointed out some years ago that there are basically two mechanisms that could be thought of by which to make them. One was the method mentioned by Hundhausen—that is, by increasing velocity in the driver gas. Another one is by the interaction of the shock wave with a tangential discontinuity, so that there is one wave reflected and one transmitted; under certain conditions the reflected wave will be a shock wave.

M. Dryer I want to ask one question and make one comment. I'm a bit puzzled about the question of the mass coming out from the sun, and thought there might be a contradiction in what was said in the first part of the talk, namely, about the gas being compressed and then later making an experimental integration of the mass and then saying that all of the mass came from the sun.

A. J. Hundhausen The whole point is if you had a steady ambient solar wind and put a blip in it all of it will eventually come out. So you continuously integrate and you have subtracted the ambient off correctly. You don't have to identify which is compressed gas and which is the original because the total ultimately passes through the sphere. The trick is that you subtracted the ambient off.

M. Dryer Except you're making a readjustment in the density distribution of that mass.

A. J. Hundhausen Yes, I'm just obtaining an integral. Now, of course, it's an estimate of the mass and energy. You would have to know what the real ambient value was and of course you don't know because it's been swept up, so one assumes it's the same as just before the shock. That's one of the limitations in the accuracy of the calculation.

M. Dryer The basis for the question was the suggestion by Hirshberg that the enriched helium represented the flare ejecta that followed the first shock by a number of hours.

A. J. Hundhausen In that case, including only that material, you get just about the same answer.

M. Dryer The second point is the comment regarding the type II radio bursts. May I show one slide (fig. 1) which is of a type II radio burst published by *Smerd* [1970] using the 80-MHz radio heliograph at Culgoora. This type II burst, which extends over more than 180° came from a flare that occurred about 20° behind the west limb. It would be very interesting if there is any information at 1 AU following this flare. The point I want to make is that this may be anomalous, but it is very suggestive that the use of spherical models is not too bad.

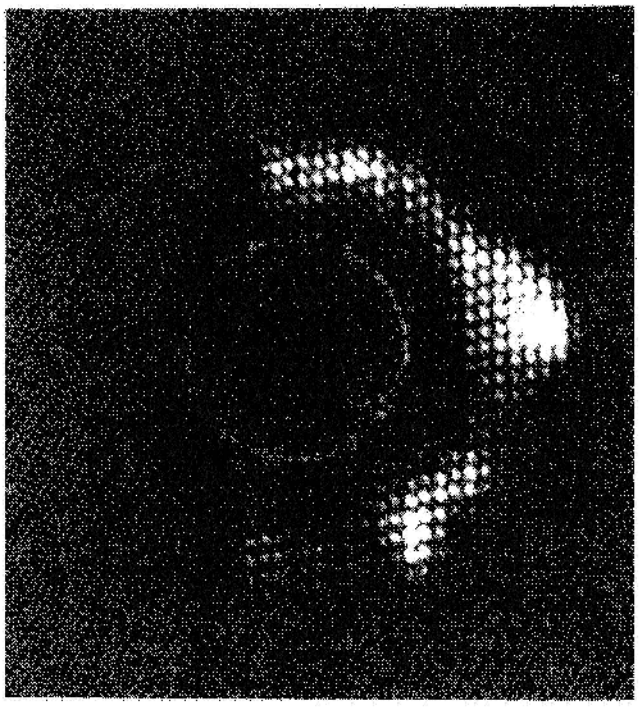

Figure 1 *Radioheliogram (Culgoora, Australia), at 80 MHz, of a series of type II radio bursts following a flare beyond the west limb on 30 March 1969, 0250 UT [Smerd, 1970].*

A. J. Hundhausen How do you know where this is along your line of sight?

M. Dryer There were some time developments of this, and so I can't really say. This radio heliogram is in the plane perpendicular to the line of sight.

J. Hirshberg I did want to mention there is a small amount of magnetic field data when we suspect ejecta is being seen; in the very few cases looked at the field does not lie in the plane of the equator of the sun but makes very large angles as you would expect.

A. J. Hundhausen You have complicated the problem by making it truly three dimensional. What I really should have said is there is no consistent idea about how the variation within the blob really goes.

J. Hirshberg Well, we haven't really been able to look back to see whether it closes or continues to be connected.

P. McIntosh I know that at least two of the events in your list were white light flares with visible shock waves in H α. Now, since white light flares are surely a bit deeper than the other flares, doesn't this allow you to get a little more particle ejecta than in the normal flare?

A. J. Hundhausen I must confess that I have in the past appeared as a skeptic regarding everybody's flare associations. This is the closest I have ever gotten to seeing anything definite. I think that any study of these observations has to be made very carefully. In fact, if they are white light flares you may be able to estimate the energy since that is the major source of energy emission other than the interplanetary shock wave; that's a fruitful thing to study.

R. J. Hynds Do I understand that if you put in the observed shock velocity near the earth, then work out the transit times, you get good agreement between the measures? Because I remember someone some years ago did a mean transit time and he came out with about 40 hr, which implies a mean velocity of about 1000 km, which implies that over a large fraction of an AU it is presumably moving at several 1000 km.

A. J. Hundhausen If you use 1 AU, of course, you imply something like 80 hr. The associations I've got are on the order of 60 or 70 hr, which I don't think is too bad an agreement. Remember that the shock wave can be moving faster close to the sun and in fact some of the observations indicate 1000 km/sec. I think that's roughly what you get from the type II bursts. If waves of the mass and energy that we have determined here do start at 1000 km/sec they are very quickly slowed down in passing through the denser parts of the corona and come out near 500 km/sec most of the way, which I think explains why the difference isn't too great. There may be some deceleration on the way out.

Unidentified Speaker The shortest transit time observed is about 16 hr. Could you then cope with such an extreme example?

A. J. Hundhausen No. That's why I'm skeptical about flare associations.

P. A. Sturrock I would like to comment on the mass problem. One has the problem of trying to understand both the source of the energy and the source of the mass in a flare. We don't know where the mass comes from, but it most probably comes from the chromosphere, not the corona. On the other hand, the magnetic energy is stored primarily in the corona, not the chromosphere. I think this paradox is related to the problem of understanding hard and soft X-ray bursts. A picture that has emerged recently is as follows: The beginning of the magnetic field reconnection gives rise to a stream of high energy particles. When these impinge on the chromosphere, they give rise to the hard X-ray bursts. They also evaporate a large mass of gas, which then gives rise to the soft X-ray burst. I suggest that the evaporation extends slightly ahead of the reconnection. Then that part of the plasma becomes trapped in the closed magnetic field lines, giving the soft X-rays, and part of the plasma is trapped in the reconnected open magnetic field lines and is subsequently ejected from the sun. Some confirmation of this hypothesis is provided by the fact that the mass of gas needed to explain the soft X-ray burst of a large flare is comparable with the mass of gas needed to explain a flare-produced shock wave in the solar wind.

Unidentified Speaker As far as accounting for the effects, I suggest that we already

have some evidence in the comparison of magnetic fields and type III bursts. We do see examples where these are channeled by the magnetic field.

T. G. Cowling Can one imagine a burst that does not proceed radially out and so that one would expect to have a certain proportion of the bursts missing the places immediately above the point of origin. One does know that something of that sort seems to effect cosmic ray eruptions from flares. I was wondering if there was anything similar in regard to ordinary flares. And whether there might be some radio observations that might support such an effect.

J. Hirshberg One of these shocks we are talking about caused a geomagnetic storm. So if we are getting things shooting out in one direction in any systematic way in the same manner, for example, as cosmic rays, we should see some east-west asymmetry in the geomagnetic storm sudden commencements, and we don't see more than a degree or two.